UNIVERSIDAD SAN FRANCISCO DE QUITO USFQ

Colegio de Ciencias e Ingenierías

Flat slabs in eccentric punching shear: experimental database and analysis

Artículo Académico

.

Daniel Eduardo Vargas Sánchez

Ingeniería Civil

Trabajo de titulación presentado como requisito
para la obtención del título de
Ingeniero Civil

Quito, 02 de mayo de 2019

UNIVERSIDAD SAN FRANCISCO DE QUITO USFQ

COLEGIO CIENCIAS E INGENIERÍAS

HOJA DE CALIFICACIÓN
DE TRABAJO DE TITULACIÓN

Flat slabs in eccentric punching shear: experimental database and analysis

Daniel Eduardo Vargas Sánchez

Calificación:

Nombre del profesor, Título académico: PhD. Eva Lantsoght

Firma del profesor: ______________________________

Quito, 02 de mayo de 2019

Derechos de Autor

Por medio del presente documento certifico que he leído todas las Políticas y Manuales de la Universidad San Francisco de Quito USFQ, incluyendo la Política de Propiedad Intelectual USFQ, y estoy de acuerdo con su contenido, por lo que los derechos de propiedad intelectual del presente trabajo quedan sujetos a lo dispuesto en esas Políticas.

Asimismo, autorizo a la USFQ para que realice la digitalización y publicación de este trabajo en el repositorio virtual, de conformidad a lo dispuesto en el Art. 144 de la Ley Orgánica de Educación Superior.

Firma del estudiante: ____

Nombres y apellidos: Daniel Eduardo Vargas Sánchez

Código: 00125120

Cédula de Identidad: 1718027723

Lugar y fecha: Quito, 02 de mayo de 2019

RESUMEN

La falla por punzonamiento excéntrico puede ocurrir en conexiones losa-columna cuando la conexión está sometida a momentos desbalanceados. Normalmente, esta situación se produce en las columnas de borde y de esquina y, por lo tanto, es un caso práctico común. Sin embargo, la mayoría de los experimentos de punzonamiento disponibles en la literatura son experimentos de naturaleza concéntrica. Este documento presenta una base de datos de 66 experimentos sobre losas planas bajo falla por punzonamiento excéntrico, incluyendo un breve resumen del procedimiento de prueba de cada referencia y una descripción de las muestras de losa. Adicionalmente, se incluye un análisis de elementos finitos lineales de todas las muestras para determinar las fuerzas internas y los momentos relevantes. Por último, la capacidad medida de los experimentos de la base de datos se comparan con las capacidades por punzonamiento determinadas con el ACI 318-14, el Eurocode 2 NEN-EN 1992-1-1:2005, *fib* Model Code 2010 y el Critical Shear Crack Theory. El resultado de esta comparación muestra que el *fib* Model Code 2010 es el modelo más preciso con una relación prueba versus pronóstico promedio de 1,26 y un coeficiente de variación de 34%. Se puede concluir que este estudio representa las inconsistencias de los métodos actualmente utilizados y la falta de información experimental.

Palabras clave: base de datos; punzonamiento excéntrico; losas planas; concreto reforzado; cortante; experimentos

ABSTRACT

Eccentric punching shear can occur in concrete slab-column connections when the connection is subjected to shear and unbalanced moments. Typically, this situation results at edge and corner columns, and is thus a common practical case. However, most punching experiments in the literature are concentric punching shear experiments. This paper presents a database of sixty-six experiments on flat slabs under eccentric punching shear, including a brief summary of the testing procedure of each reference and a description of the slab specimens. Additionally, a linear finite element analysis of all the specimens is included to determine the relevant sectional shear forces and moments. Finally, the ultimate shear stresses from the database experiments are compared to the shear capacities determined with the ACI 318-14, Eurocode 2 NEN-EN 1992-1-1:2005, Model Code 2010, and the Critical Shear Crack Theory. The result of this comparison shows that the Model Code 2010 is the most precise model with an average predicted shear of 1.26 and a coefficient of variation of 34%. It can be concluded that this study represents the inconsistencies of the currently used methods and the lack of experimental information.

Keywords: database; eccentric punching shear; experiments; flat slab; punching; reinforced concrete; shear; shear reinforcement

TABLA DE CONTENIDO

materials

Article

Flat slabs in eccentric punching shear: experimental database and analysis

Daniel Vargas [1*], Eva O.L. Lantsoght[1,2], Katerina Genikomsou[3]

[1] Politécnico, Universidad San Francisco de Quito, Quito 170901, Ecuador
[2] Concrete Structures, Department of Engineering Structures, Civil Engineering and Geosciences, Delft University of Technology
[3] Queen's University, Kingston, ON, Canada
* Correspondence: danielvargas2901@gmail.com; Tel.: +593 999 757 470

Received: date; Accepted: date; Published: date

Abstract: Eccentric punching shear can occur in concrete slab-column connections when the connection is subjected to shear and unbalanced moments. Typically, this situation results at edge and corner columns, and is thus a common practical case. However, most punching experiments in the literature are concentric punching shear experiments. This paper presents a database of sixty-six experiments on flat slabs under eccentric punching shear, including a brief summary of the testing procedure of each reference and a description of the slab specimens. Additionally, a linear finite element analysis of all the specimens is included to determine the relevant sectional shear forces and moments. Finally, the ultimate shear stresses from the database experiments are compared to the shear capacities determined with the ACI 318-14, Eurocode 2 NEN-EN 1992-1-1:2005, Model Code 2010, and the Critical Shear Crack Theory. The result of this comparison shows that the Model Code 2010 is the most precise model with an average predicted shear of 1.26 and a coefficient of variation of 34%. It can be concluded that this study represents the inconsistencies of the currently used methods and the lack of experimental information.

Keywords: database; eccentric punching shear; experiments; flat slab; punching; reinforced concrete; shear; shear reinforcement

1. Introduction

Structural concrete flat slabs are an interesting solution for building design due to the simplicity of the construction process and the associated (economical) advantages. Nevertheless, a difficulty lies in the uncertainty of predicting slab-column connection behavior and capacity when lateral loads or unbalanced gravity loads cause a transfer of moments between the slab and the column [1]. Such moments can also be caused by asymmetrical spans, creep, and differential shrinkage between two continuous slabs [2].

An important number of collapses caused by punching failure have been reported throughout the years, which gained the attention of researchers and practitioners [3]. One example of the most representative cases is the collapse of the underground parking garage in Gretzenbach, Switzerland on November 2004 [4]. The collapsed structure had no shear reinforcement, only column capitals were provided as a shear enhancement resource. This collapse caused the dead of seven men.

Typically, the most critical slab-column connections are located on corners and edges as these connections are subjected to moment transfer and eccentric loading. However, these are the less studied in comparison with internal slab-column connections.

This work aims to present a wider view of the problem by compiling and analyzing information from different authors on eccentric punching shear. The analysis of the compiled experiments can be used to analyze the performance of the currently available building codes and identify which types of experiments would be a valuable contribution to the body of knowledge. Additional experiments could be used to refine and improve the existing models.

The first coherent studies on punching shear were made in the 1960s by Kinnunen and Nylander [5], but their mechanical models resulted in complicated expressions, which the codes found unpractical to use [6]. Instead, empirical expressions were developed. Given that there is a lack of experimental information on eccentric punching shear on large scale flat slabs, it becomes difficult to provide a satisfactory design expression [2]. To account for eccentric loading, the ACI 318-14 [7] and Eurocode 2 EN 1992-1-1:2005 [8] models use a factored shear stress on the critical perimeter. On the other hand, the *fib* Model Code 2010 [9] and the Critical Shear Crack Theory [10,11] use a reduction of the critical perimeter.

This article compiles 66 experiments on flat slabs in eccentric punching shear. Vertical, horizontal and combined loading setups are reported in the literature. Both slabs with and without shear reinforcement are included in the database. Internal forces of the slabs for the maximum applied load, i.e. at the onset of punching shear failure, and elementary design magnitudes are typically not available in the references. To complete the missing information, a linear finite element model of each specimen is made. The experimental shear capacities from the database are then compared to the strengths predicted by the design expressions found in ACI 318-14 [7], Eurocode 2 NEN-EN 1992-1-1:2005 [8], *fib* Model Code 2010 [9] and the Critical Shear Crack Theory [10,11].

2. Methods

2.1 Overview of code provisions

2.1.1 ACI 318 – 14

The punching shear provisions from ACI 318-14 are empirical equations resulting from the work of Moe [12] and ACI-ASCE Committee 426 [13]. The ACI 318-14 method is based on the maximum shear stress v_u on the critical perimeter b_o of the slab, which is located at 0.5d from the face of the column, where d is the average slab effective depth. The maximum shear stress v_u should not exceed the nominal shear strength of the slab v_n. The ACI 318-14 §8.4.1.1 expresses that it is necessary to consider unbalanced moments, but it doesn't prescribe how this should be done. Figure 1 is a sketch of the shear stress produced by axial load and moment transfer [1].

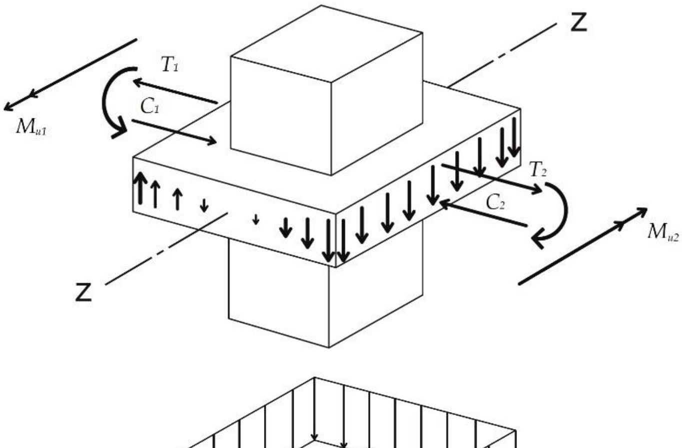

(a)

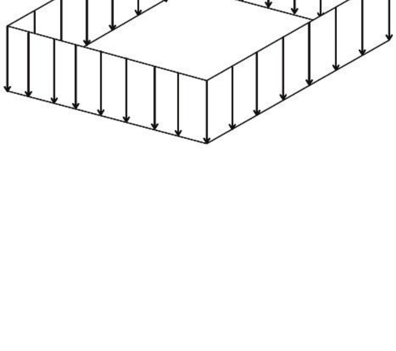

(b)

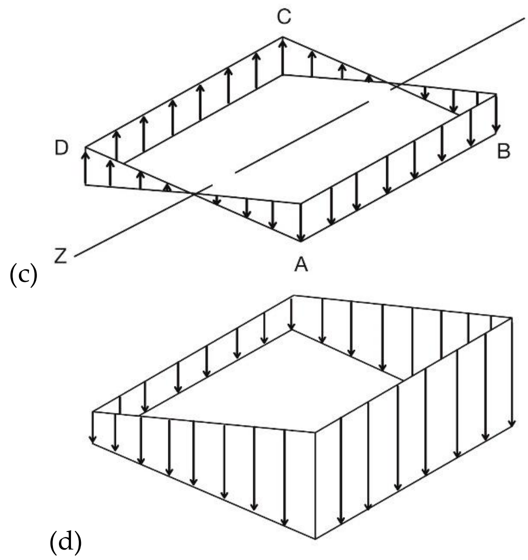

Figure 1. Shear stress produced by applied load and moment transfer, modified from [1]: (a) transfer of unbalanced moments to column; (b) shear stress caused by direct shear; (c) shear stress caused by unbalanced moments; (d) total shear stress: sum of (b) and (c).

MacGregor and Wight [1] define v_u using the following equation:

$$v_u = \frac{V_u}{b_o d} \pm \frac{\gamma_v M_{u1} C}{J_{c1}} \pm \frac{\gamma_v M_{u2} C}{J_{c2}} \quad (1)$$

where V_u is the factored shear being transferred from the slab to the column acting on the centroid of the critical section; c is the distance from the centroid of the critical section to the point where the shear stress is calculated; J_c is the polar moment of inertia of the critical section and $\gamma_v M_u$ is the fraction of moment transferred by eccentricity of shear, with γ_v as follows:

$$\gamma_v = 1 - \gamma_f \quad (2)$$

where γ_f is the fraction of moment transmitted by flexure:

$$\gamma_f = \frac{1}{1 + \left(\frac{2}{3}\right)\sqrt{\frac{b_1}{b_2}}} \quad (3)$$

where b_1 is the total width of the critical section measured perpendicular to the axis about which the moment acts, and b_2 is the total width parallel to the axis [1]. Figure 2 shows a sketch of the critical perimeter of an interior, edge, and corner slab-column connection.

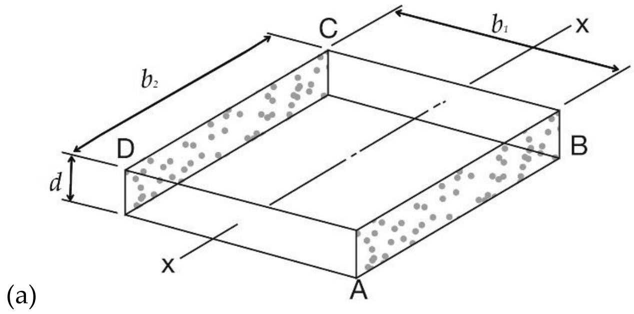

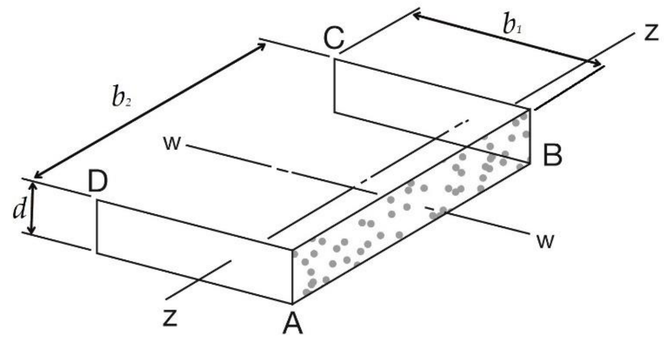

(b)

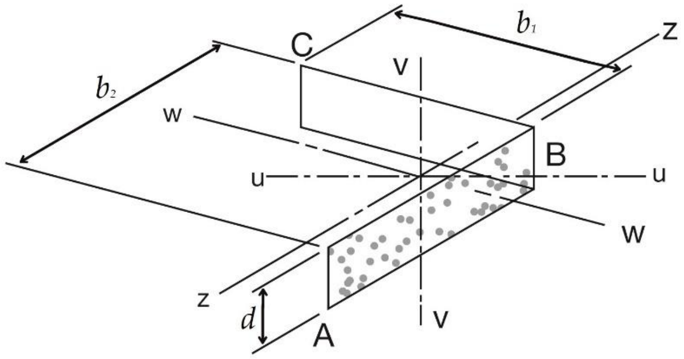

(c)

Figure 2. Critical perimeter of an interior, edge and corner slab-column connections, modified from [1]: (a) interior slab-column connection; (b) edge slab-column connection; (c) corner slab-column connection.

The polar moment of inertia J_c can be calculated as follows:

$$J_c = 2\left(\frac{b_1 d^3}{12} + \frac{d b_1^3}{12}\right) + 2(b_2 d)\left(\frac{b_1}{2}\right)^2 \quad \text{for an interior slab-column connection} \tag{4}$$

$$J_c = 2\left[\frac{b_1 d^3}{12} + \frac{d b_1^3}{12} + (b_1 d)\left(\frac{b_1}{2} - C_{AB}\right)^2\right] + b_2 d C_{AB}^2 \quad \text{for an edge slab-column connection} \tag{5}$$

$$J_c = \left[\frac{b_1 d^3}{12} + \frac{d b_1^3}{12} + (b_1 d)\left(\frac{b_1}{2} - C_{AB}\right)^2\right] + b_2 d C_{AB}^2 \quad \text{for a corner slab-column connection} \tag{6}$$

where C_{AB} is the distance to the centroid of the critical perimeter:

$$C_{AB} = \frac{(b_1 d) b_1}{2(b_1 d) + b_2 d} \quad \text{for an edge slab-column connection} \tag{7}$$

$$C_{AB} = \frac{(b_1 d) b_1 / 2}{b_1 d + b_2 d} \quad \text{for a corner slab-column connection} \tag{8}$$

According to ACI 318-14 section 22.6.5.2 [7] in slabs without shear reinforcement, the shear stress shall not exceed the least of the following three expressions, with f_c' in [MPa].

$$v_c = 0.33\lambda\sqrt{f_c'} \tag{9}$$

$$v_c = 0.17\left(1 + \frac{2}{\beta}\right)\lambda\sqrt{f_c'} \tag{10}$$

$$v_c = 0.083\left(2 + \frac{\alpha_s d}{b_o}\right)\lambda\sqrt{f_c^{'}} \tag{11}$$

The value of α_s is 40 for interior columns, 30 for edge columns, and 20 for corner columns; λ is the lightweight factor; and β is the ratio of long to short directions of the critical perimeter [7]. Section 22.6.6.1 [7] indicates that the value of v_c for shear reinforced slabs shall not exceed the following:

$$v_c = 0.17\lambda\sqrt{f_c^{'}} \tag{12}$$

$$v_c = 0.25\lambda\sqrt{f_c^{'}} \tag{13}$$

Eq. (12) is used for stirrup reinforcement and Eq. (13) is used for headed shear stud reinforcement. When shear reinforcement is used, the critical perimeter b_o shall be taken outside the reinforced section as illustrated in Figure 3 [7].

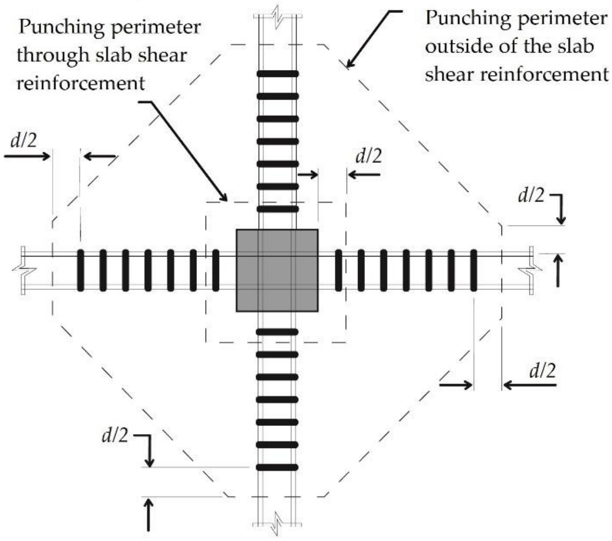

(a)

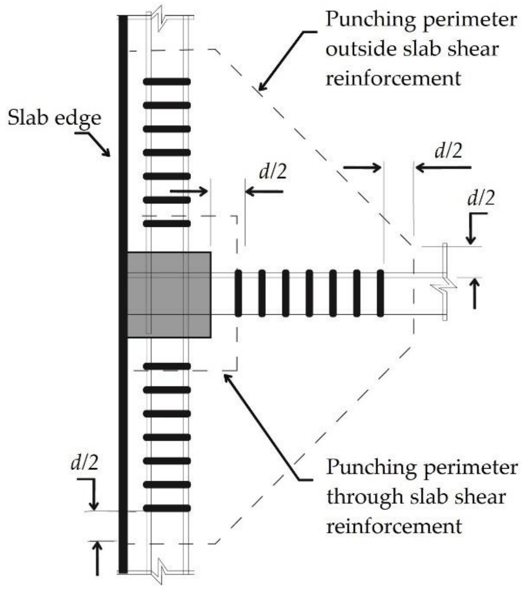

(b)

(c)
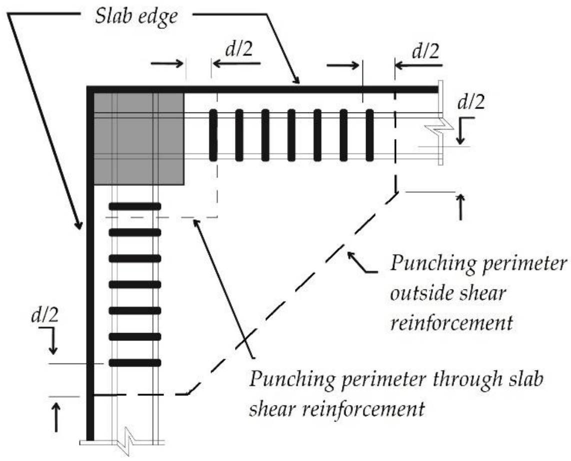

Figure 3. Critical perimeter for a shear reinforced interior, edge, and corner slab-column connection, modified from [7]: (a) interior slab-column connection; (b) edge slab-column connection; (c) corner slab-column connection.

The contribution of the shear reinforcement v_s is determined as:

$$v_s = \frac{A_v f_{yt}}{b_o s} \quad (14)$$

where A_v is the sum of the area of all legs of reinforcement on the peripheral line that is geometrically like the perimeter of the column section, f_{yt} is the yield strength of the transverse reinforcement and s is the spacing of transversal reinforcement [7]. The ultimate shear capacity v_n is calculated as follows, with v_u as determined by Eq. (1):

$$v_n = v_c + v_s \geq v_u \quad (15)$$

2.1.2 NEN-EN 1992-1-1:2005

The punching shear provisions of NEN-EN 1992-1-1:2005 contain empirical equations for the concrete contribution to the two-way shear capacity. It is assumed that the concrete contribution to the shear capacity is equal for one-way shear (beam shear) and two-way shear (punching shear).

According to the provisions of NEN-EN 1992-1-1:2005 [8] punching shear is checked at the basic control perimeter U_1. The basic control perimeter U_1 is located at $2d$ from the loaded area, with d the average effective depth of the slab. Figure 4 shows the basic control perimeter for an interior, edge, and corner slab-column connection [8]. Note that rounded corners are used for the perimeter.

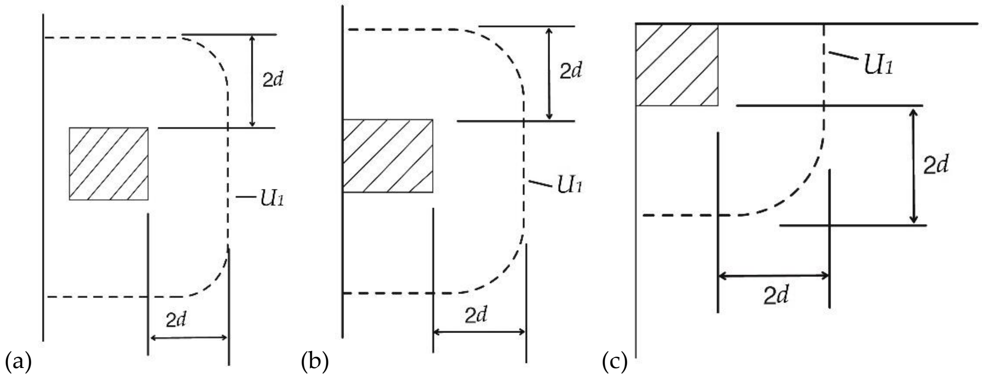

Figure 4. Basic control perimeter for an interior, edge, and corner slab-column connection, modified forms [8]: (a) interior slab-column connection; (b) edge slab-column connection; (c) corner slab-column connection.

Punching shear is evaluated based on the following stresses: $v_{Rd,c}$ the design value of the punching shear resistance of a slab without punching shear reinforcement, $v_{Rd,s}$ the value of the punching shear resistance of a slab with punching shear reinforcement, and v_{Ed} the maximum shear stress along the control section. If $v_{Ed} \leq v_{Rd,c}$ punching shear reinforcement is not necessary. If the support reaction is eccentric with respect to the control perimeter, the maximum shear stress is:

$$v_{Ed} = \beta \frac{V_{Ed}}{U_1 d} \tag{16}$$

$$\beta = 1 + k_c \frac{M_{Ed}}{V_{Ed}} \frac{U_1}{W_1} \tag{17}$$

where W_1 represents the shear distribution on the control perimeter, V_{Ed} is the design value of the applied shear force, M_{Ed} is the design value of the applied bending moment, and k_c is a coefficient on the ratio between the column dimensions given by Table 6.1 of NEN-EN 1992-1-1:2005 [8]. A few values of k_c are 0.6 for a c_1/c_2 ratio of 1.0 and 0.70 for a c_1/c_2 ratio of 2.0. Where c_1 and c_2 are the dimensions of the critical perimeter, see Figure 5. W_1 is calculated as:

$$W_1 = \int_0^{u_i} |e| \, dl \tag{18}$$

where U_i is the length of the control perimeter under consideration, dl is a length increment of the perimeter, and e is the distance of dl from the axis about which the moment M_{Ed} acts [8]. Figure 5 shows the shear distribution due to an unbalanced moment at a slab-column connection.

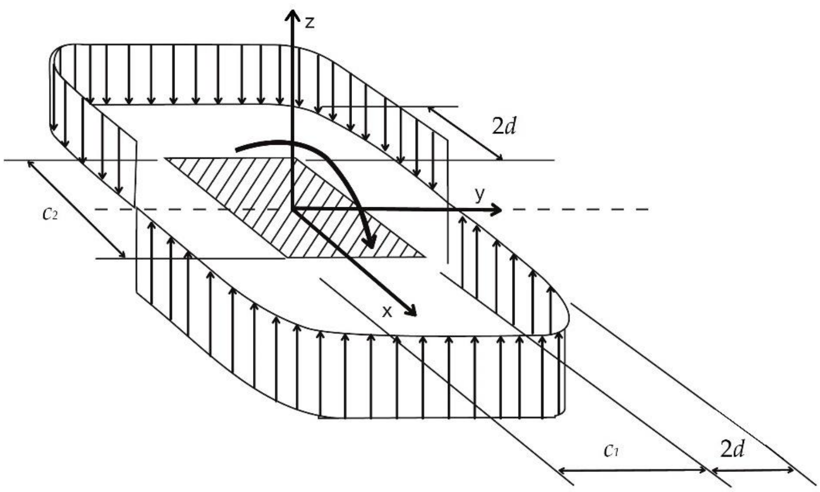

Figure 5. Shear distribution due to an unbalanced moment at a slab-column connection, modified from [8].

For an internal rectangular column where the loading is eccentric to both orthogonal axes, β shall be calculated as follows:

$$\beta = 1 + 1.8\sqrt{\left(\frac{e_y}{b_x}\right)^2 + \left(\frac{e_x}{b_y}\right)^2} \tag{19}$$

Where e_y and e_x are the eccentricities M_{Ed}/V_{Ed} along the axes y and x respectively and b_x and b_y are the dimensions of the control perimeter. For edge slab-column connections, where the eccentricity is perpendicular to the slab edge is towards the interior and there is no eccentricity parallel to the edge, the control perimeter may be reduced to U_1^* as illustrated in Figure 6a. For corner slab-column connections, where the eccentricity is towards the interior of the slab, the control perimeter may be reduced to U_1^* as illustrated in Figure 6b [8].

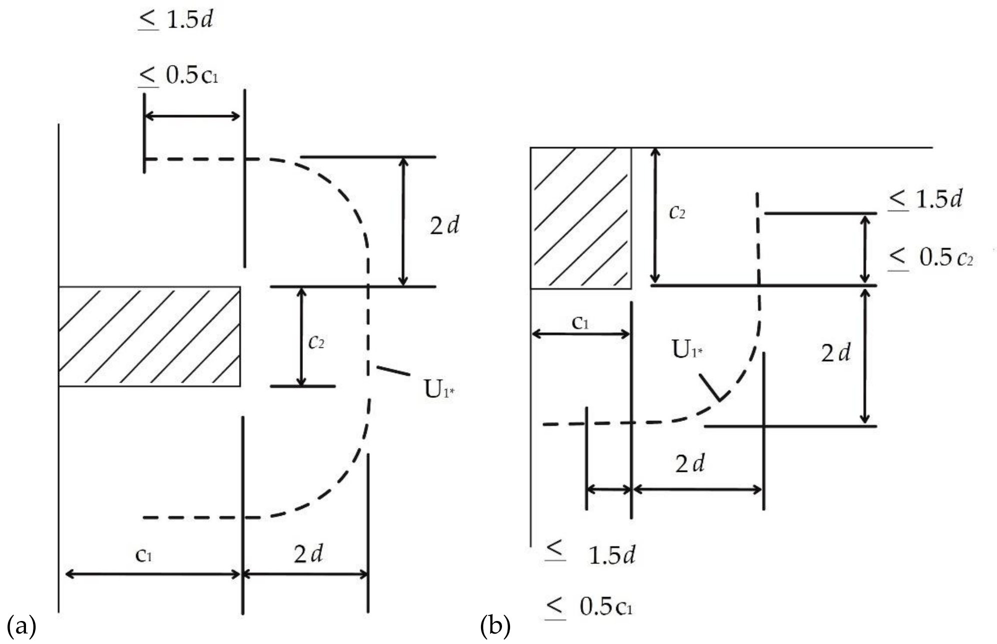

Figure 6. Reduced basic control perimeter, modified from [8]: (a) edge slab-column connection; (b) corner slab-column connection.

For edge slab-column connections, if there are eccentricities in both orthogonal directions, β shall be calculated as:

$$\beta = \frac{U_1}{U_1^*} + k_c \frac{U_1}{W_1} e_{par} \tag{20}$$

where e_{par} is the eccentricity parallel to the slab edge. For corner column connections, where the eccentricity is toward the interior of the slab, β shall be calculated as

$$\beta = \frac{U_1}{U_1^*} \tag{21}$$

If the eccentricity is towards the exterior, β shall be calculated using equation Eq. (19). For practical purposes, W_1 shall be calculated as:

$$W_1 = \frac{c_1^2}{2} + c_1 c_2 + 4c_2 d + 16d^2 + 2\pi d c_1 \text{ for a rectangular interior column} \tag{22}$$

$$W_1 = \frac{c_1^2}{4} + c_1 c_2 + 4c_1 d + 8d^2 + \pi d c_2 \text{ for a rectangular edge column} \tag{23}$$

$$W_1 = \frac{c_1 c_2}{2} + 2c_1 d + \frac{c_2^2}{4} + 4d^2 + \frac{\pi d c_2}{2} \text{ for a rectangular corner column} \tag{24}$$

The punching shear resistance of slabs without shear reinforcement is $v_{Rd,c}$:

$$v_{Rd,c} = C_{Rd,c} k (100 \rho_l f_{ck})^{\frac{1}{3}} \geq v_{\min} \tag{25}$$

with $C_{Rd,c}$ taken as $0.18/\gamma_c$, with γ_c the material factor for concrete (γ_c = 1.5), and k is the size effect factor

$$k = 1 + \sqrt{\frac{200}{d}} \leq 2 \text{ with } d \text{ in [mm]} \tag{26}$$

The reinforcement ratio is the geometric average of the reinforcement ratio in the y (ρ_{ly}) and x (ρ_{lx}) direction:

$$\rho_l = \sqrt{\rho_{lx}\rho_{ly}} \tag{27}$$

The lower bound of the shear capacity is a nationally determined parameter, with a recommended expression for v_{min} as:

$$v_{\min} = 0.035k^{3/2} f_{ck}^{\ 1/2} \text{ with } f_{ck} \text{ in [MPa]} \tag{28}$$

The punching shear resistance of slabs with shear reinforcement is calculated as:

$$v_{Rd,cs} = 0.75 v_{Rd,c} + 1.5\left(\frac{d}{s_r}\right) A_{sw} f_{ywd,ef} \left(\frac{1}{U_1 d}\right) \sin\alpha \tag{29}$$

where A_{sw} is the area of one perimeter of shear reinforcement around the column, s_r is the radial spacing of perimeters of shear reinforcement, $f_{ywd,ef}$ is the effective design strength of the punching shear reinforcement and α is the angle between shear reinforcement and the horizontal plane of the slab.

2.1.3 Model Code 2010

The *fib* Model Code 2010 punching shear provisions are based on the Critical Shear Crack Theory [10,11]. The design shear demand V_{Ed} acts on the basic control perimeter $b_{1,MC}$, at $0.5d_v$ from the supported area, where d_v is the effective depth of the slab. Figure 7 illustrates the basic control perimeter for different supported areas.

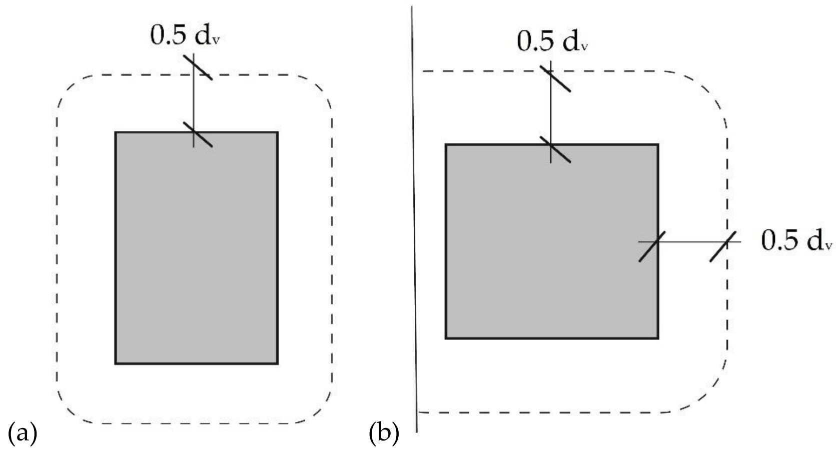

Figure 7. Basic control perimeter, modified from [9]: (a) interior column; (b) edge slab-column connection.

Then, for calculating the punching shear resistance of the slab, a shear-resisting control perimeter b_0 is used. This perimeter accounts for the non-uniform distribution of shear forces along $b_{1,MC}$, which can be caused by concentrations of the shear forces due to moment transfer between the slab and the supported area as a result of eccentricities in the load application [9]. Figure 8 illustrates the eccentricity of the resultants [9].

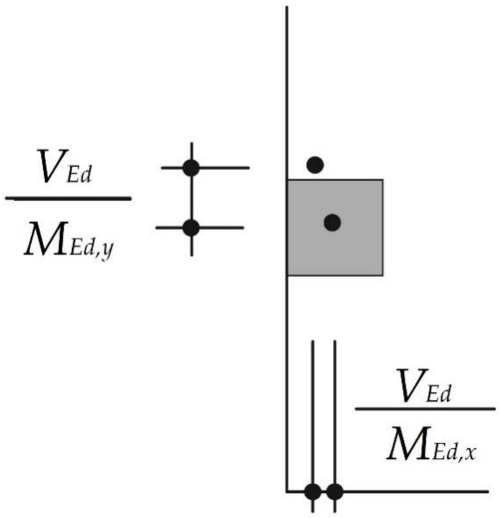

Figure 8. Resultant of shear forces, modified from [9]

The control perimeter b_0 is determined as:

$$b_0 = k_e b_{1,MC} \tag{30}$$

k_e represents the coefficient of eccentricity:

$$k_e = \frac{1}{1 + \frac{e_u}{b_u}} \tag{31}$$

where e_u is the eccentricity of the resultant shear forces with respect to the centroid of $b_{1,MC}$, and b_u is the diameter of a circle with the same area as the region inside $b_{1,MC}$. The punching shear resistance V_{Rd} is calculated as:

$$V_{Rd} = V_{Rd,c} + V_{Rd,s} \geq V_{Ed} \tag{32}$$

The design shear resistance attributed to the concrete is calculated as:

$$V_{Rd,c} = k_\psi \frac{\sqrt{f_{ck}}}{\gamma_c} b_0 d_v \quad \text{with } f_{ck} \text{ in [MPa]} \tag{33}$$

k_ψ is a parameter that depends on the rotations of the slab and shall be calculated as:

$$k_\psi = \frac{1}{1.5 + 0.9 k_{dg} \psi d} \leq 0.6 \tag{34}$$

where d is the mean value of the effective depth of the slab for x and y directions. If the maximum aggregate size d_g is greater than 16 mm, then $k_{dg} = 1$. If not, k_{dg} shall be calculated as follows:

$$k_{dg} = \frac{32}{16 + d_g} \geq 0.75 \quad \text{with } d_g \text{ in [MPa]} \tag{35}$$

The design shear resistance attributed to the shear reinforcement is calculated as:

$$V_{Rd,s} = \sum A_{sw} k_e \sigma_{swd} \sin\alpha \tag{36}$$

where $\sum A_{sw}$ is the sum of the area of all the shear reinforcement acting on the zone between $0.35d_v$ and d_v, which has a length of $0.65d_v$, see Figure 9 [9].

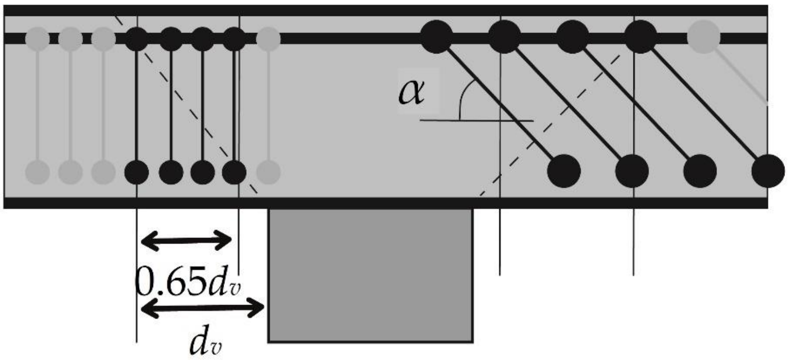

Figure 9. Shear reinforcement acting at failure, based on [9].

The stress σ_{swd} is calculated as:

$$\sigma_{swd} = \frac{E_s \psi}{6}(\sin\alpha + \cos\alpha)\left(\sin\alpha + \frac{f_{bd}}{f_{ywd}}\frac{d}{\phi_w}\right) \leq f_{ywd} \tag{37}$$

where ϕ_w represents the diameter of the shear reinforcement and f_{ywd} its yield strength. The bond strength f_{bd} is assumed to be equal to 3 MPa.

The load rotation behavior of the slab is calculated as follows:

$$\psi = 1.5\frac{r_s}{d}\frac{f_{yd}}{E_s}\left(\frac{m_{sd}}{m_{rd}}\right)^{1.5} \tag{38}$$

where r_s is the distance from the column axis to the line of contraflexure of the radial bending moments; f_{yd} is the yield strength of the flexural reinforcement, E_s the modulus of elasticity of the flexural steel, m_{sd} the average moment per unit length for calculating flexural reinforcement in the support strip, and m_{Rd} is the average flexural strength per unit length in the support strip [9]. The values of the mechanical parameters in the formula can be calculated with different levels of approximation (LoA), considering that every level of approximation represent a different grade of precision [6].

LoA I assumes that $m_{sd} = m_{Rd}$, which implies that the strength of the slab will be governed by its bending moment capacity. For regular slabs with a long over short side ratio $0.5 \leq L_x/L_y \leq 2.0$, r_s can be estimated as follows:

$$\begin{aligned} r_{sx} &= 0.22L_x \\ r_{sy} &= 0.22L_y \end{aligned} \tag{39}$$

Figure 10 illustrates L_x and L_y [9].

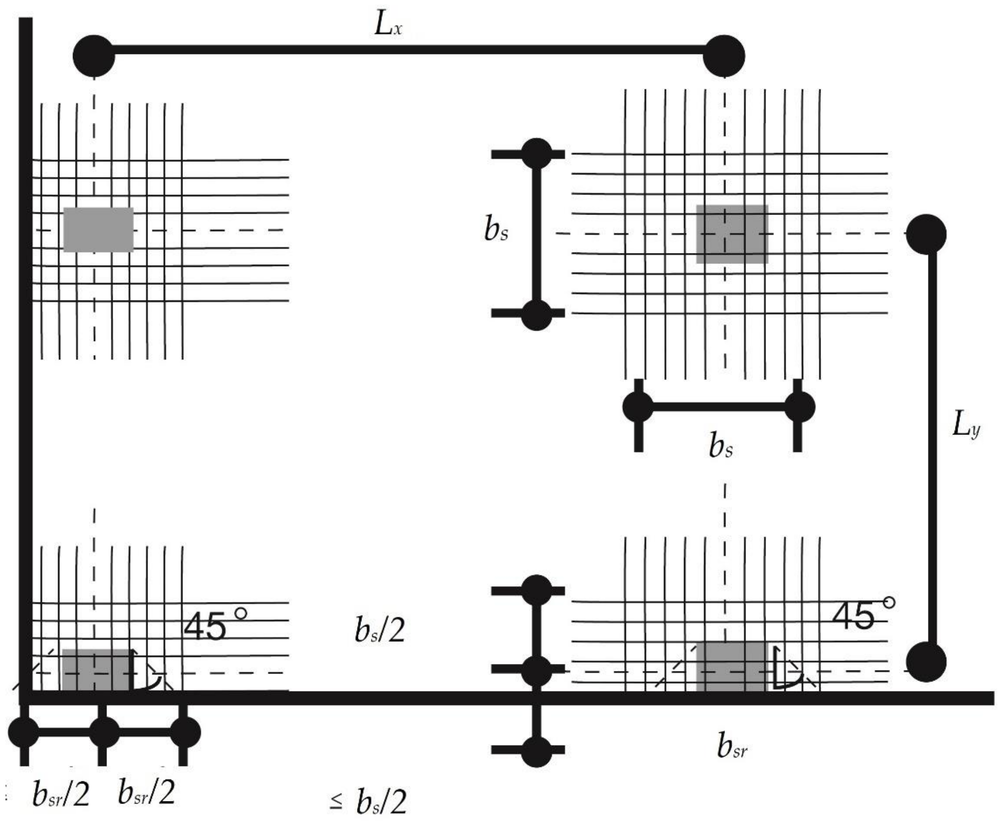

Figure 10. Slab dimensions, modified from [9].

LoA II includes a simplified of estimation m_{sd}

$$m_{sd} = V_{Ed}\left(\frac{1}{8} + \frac{e_u}{2b_s}\right) \tag{40}$$

where $2b_s$ is the width where the transferred moment acts. Considering that half of the moment acts on each side of the column [6], b_{sr} is the width of the support strip for corner and edge slabs. LoA II considers a significant bending moment redistribution in design [9]. This LoA is recommended for irregular slabs where L_x/L_y is not between 0.5 and 2.0 [9].

LoA III takes the coefficient 1.5 in Eq. (38) and replace it by 1.2 if r_s and m_{sd} are calculated using a linear elastic model. LoA IV is based on a nonlinear analysis of the structure and, it considers cracking, tension-stiffening effects, yielding of the reinforcement, and any other relevant nonlinear effects [9].

2.1.4 Critical Shear Crack Theory (CSCT)

For reinforced slabs, a simplified code-like formulation can be used to calculate punching shear strength within the shear-reinforced zone is as follows [10]:

$$V_{Rd} = V_{cd} + V_{sd} \tag{41}$$

The shear force carried by the concrete V_{cd} is calculated as:

$$V_{cd} = \frac{1}{\gamma_c}\frac{2}{3}\frac{b_{0,\text{int}} d\sqrt{f_{ck}}}{1 + 20\dfrac{\psi d}{d_{g0} + d_g}} \quad \text{with } f_{ck} \text{ in [MPa]} \tag{42}$$

where $b_{0,int}$ is the perimeter of the critical section inside the shear reinforced zone, d the effective depth of the slab, f_{ck} the compressive strength of the concrete, γ_c the partial safety factor of the concrete γ_c =

1.5, d_{g0} the reference aggregate size (16 mm), d_g the maximum aggregate size, and ψ the rotation of the slab.

The shear force carried by the shear reinforcement equals:

$$V_{sd} = \frac{E_s \psi}{6} A_{sw} \leq f_{ywd} A_{sw} \tag{43}$$

where A_s is the amount of shear reinforcement within a perimeter at a distance d from the edge of the support region, f_{ywd} is the design yield strength of the shear reinforcement, and E_s is modulus of elasticity.
For non-reinforced slabs, Eq. (41) is modified, making V_{sd} equal to 0, and Eq. (42) is modified, changing $b_{0,int}$ for the control perimeter b_0 defined in Figure 7.

2.2 Database of experiments

2.2.1 Development of database

The database developed for this study contains 66 experiments of eccentric punching shear on flat slabs with longitudinal reinforcement and with or without transverse shear reinforcement reported in the literature. The consulted references are Krüger [2], Albuquerque et al [14], Hammill and Ghali [15], Narashimhan [16], Zaghlool [17], Anis [18] and Tankut [19]. Tables A1-A3 present the database developed for this study. The full spreadsheet is available in the public domain in .xlsx format [20]. The notations used in this database are given in the "List of notations". Figure 11 illustrates the different slab geometries and slab-column connections found in the literature [2,16,17].

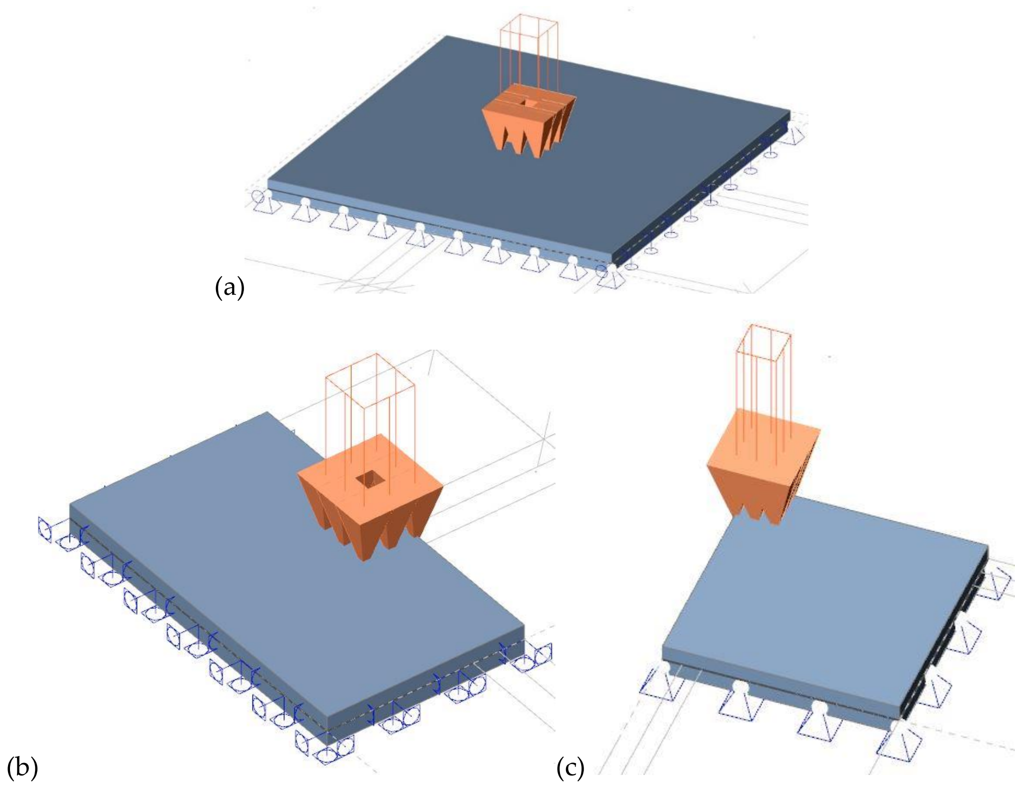
(a) (b) (c)

Figure 11. Slab geometries and test slab-column connection: (a) square interior slab-column connection [2]; (b) rectangular edge slab-column connection [16]; (c) square corner slab-column connection [17].

Reference [14] does not present the dimensions of the hard rubber pads that transmit the force from the hydraulic jacks to the slab; square pads of 100 mm × 100 mm are assumed based on the figures presented in the original reference. Reference [17] doesn't report the width of the slab support; a 100 mm width is estimated based on the provided drawings. The specimens in reference [19] are not supported like the other slabs. Since the author tested two continuous slabs representing an actual building floor, the width of the support is taken as 0 mm for this reference, as only the slab-column connection is evaluated for this work.

The age of the specimens at testing is not given by the references [2,14,15]; 28 days is assumed. The tensile strength of the concrete f_{ct} is calculated for the references that don't present this information [2,15,18,19] from the average compressive strength f_c with the expression developed from Sarveghadi [21]:

$$f_{ct} = 0.76\sqrt{f_c} \text{ with } f_c \text{ in [MPa]} \tag{44}$$

For references [2,15,19], the maximum aggregate size is assumed to be 9.5 mm.

For references [14,15,18,19], the spacing of the longitudinal reinforcement is taken from the technical drawings in the papers, or as the average spacing of the bars when the reinforcement layout is too complex. The number of bars for flexural reinforcement of the reference [18] was estimated from the drawings provided by the author. For references [2,15] the modulus of elasticity of the reinforcing steel E_s is assumed to be 200 GPa. References [2,14,15,16] present slabs with transverse shear reinforcement: stirrups, shear hats (see Figure 12), and studs were the shear reinforcement types found in these references. Table A4 presents the database for shear reinforced specimens.

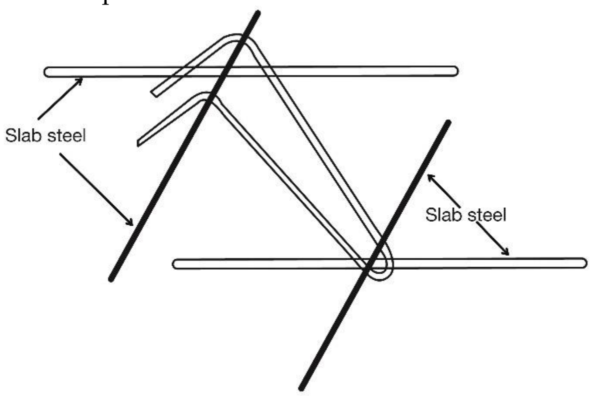

Figure 12. Shear hat setup, as used in [16].

The results are reported as the ultimate load applied to the slab-column connection and its moment caused by the eccentricity. References [2,14,16] don't give the moments transmitted to the slab by the columns. For these references, the bending moments are calculated using the applied load and the reported eccentricity. References [15,17] use a diagonal moment on the x-y axis on the square corner slabs. Figure 13 illustrates this type of loading.

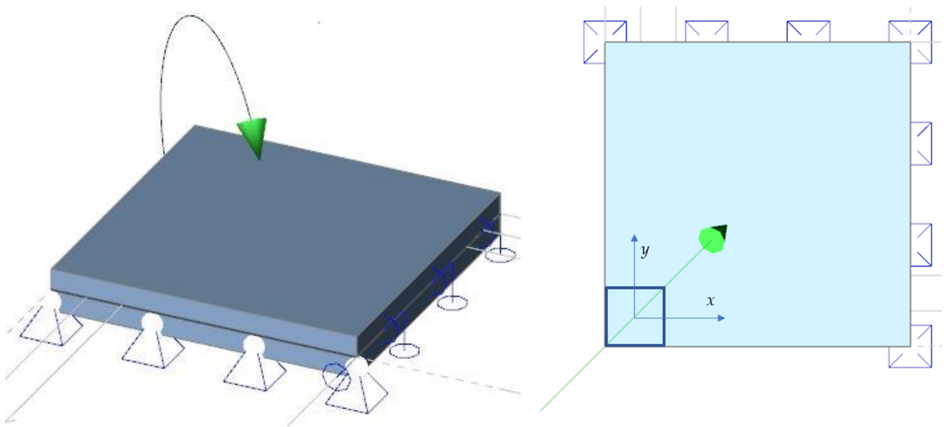

Figure 13. Diagonal loading setup.

For the database in Table A3, the diagonally applied moment was divided into its components in the x- and y-directions. Reference [14] presents the sectional shear force V_u caused by the applied load, neglecting the contribution of the self-weight of the slabs. All reported values for the sectional shear force at failure V_u in the database include the contribution of the self-weight when testing occurred in the gravity direction (i.e. self-weight increases sectional shear). For the references [2,14,19] the self-weight of the slabs was included in the analysis. Where the internal forces at failure were not found in the original reference, the linear finite element program SCIA Engineer [22] was employed to obtain sectional shear forces and moments, and elementary design magnitudes, see Figure 14. Special care on the type of support used in the model slabs was taken, as normal forces were not desired in the results. The models were as similar to the reported experiments as possible. The results presented in the Table A5 are the maximum internal forces of the slab at failure.

Most of the entries in the database failed in brittle punching shear failure. Nevertheless, references [2,14,18] present a few specimens that failed by flexure-induced punching shear.

All values in the database are presented in SI units. The information from [17,18,19] was converted from U.S customary units to SI units.

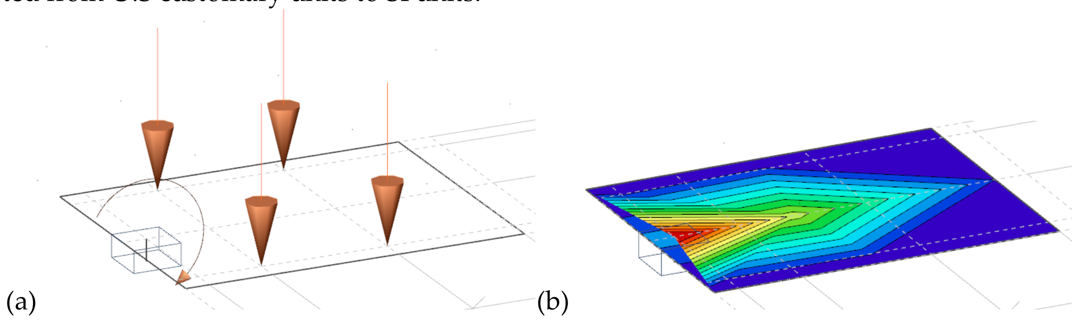

Figure 14. Example of Finite Element Analysis on an Albuquerque [14] specimen: (a) Applied loads in the model; (b) Internal force V_x calculated from the applied load and the self-weight of the specimen.

2.2.2 Parameter ranges in the database

In this section, an evaluation of the distribution of the values of the parameters in the database is made. Table 1 gives the ranges of the most important parameters in the database.

Table 1. Ranges of parameters in database

Parameter	Min	Max
h (mm)	102	180
d (mm)	76	153
L_x (mm)	762	3000
L_y (mm)	762	3000
a (mm)	400	1375
a_v (mm)	200	1100
ρ (%)	0.72%	2.40%
f_c (MPa)	26	59
a/d (-)	5.25	8.99
a_v/d (-)	2.62	7.20

Figure 15 shows the distribution of the most important parameters in the database. Figure 15a shows that the majority of slabs are made of normal strength concrete. The developed database cannot be used to gain insight in the eccentric punching shear capacity of high strength concrete slab-column connections. Figure 15b shows that a tensile reinforcement ratio close to 1.25% was commonly used in the tested slabs. Typical slab designs use reinforcement ratios of 0.6% - 0.8%. Only 5 of the experiments in the database use these practical values. Most slabs were over-reinforced in flexure to achieve a punching shear failure. The distribution of the average effective depth of the slab is presented in Figure 15c. This plot shows that most experiments had an effective depth d in the range from 100 mm to 125 mm. The reported specimens are small-scale specimens which do not give us insights regarding the size effect for eccentric punching shear. Figure 15d shows the ratio between the shear span and the average effective depth *a*/*d*. The range of *a*/*d* in the experiments covers only situations in which no direct load transfer can occur.

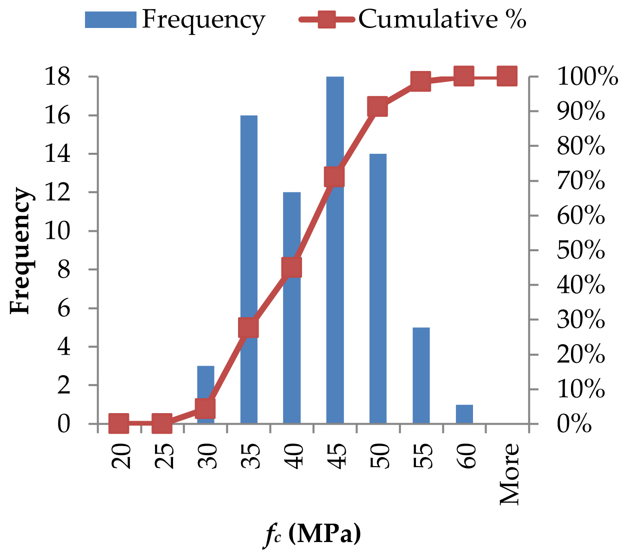

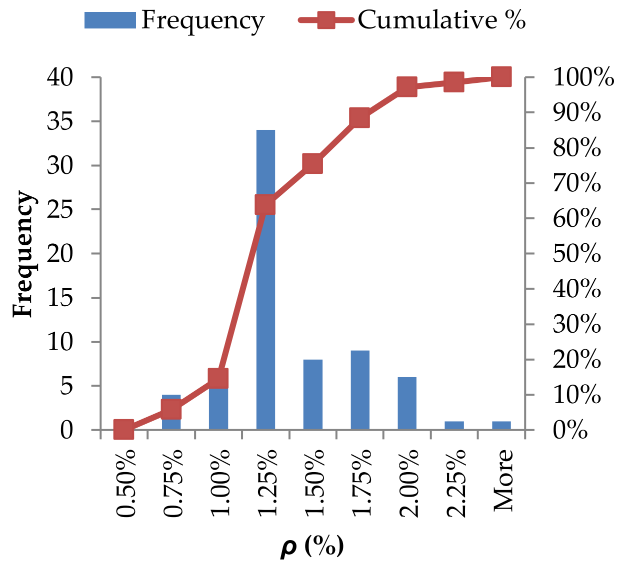

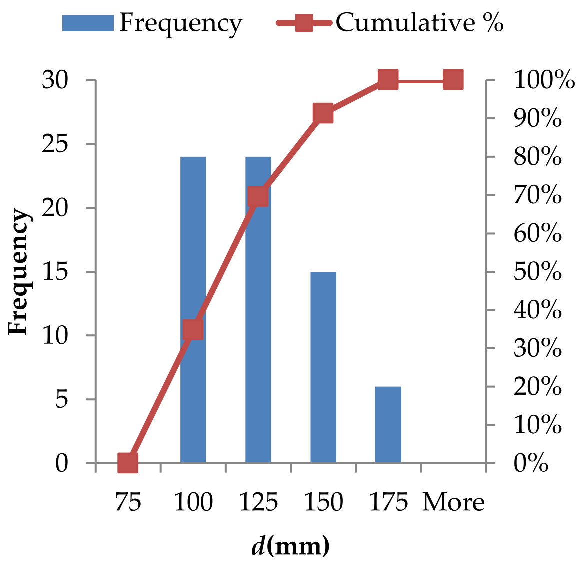

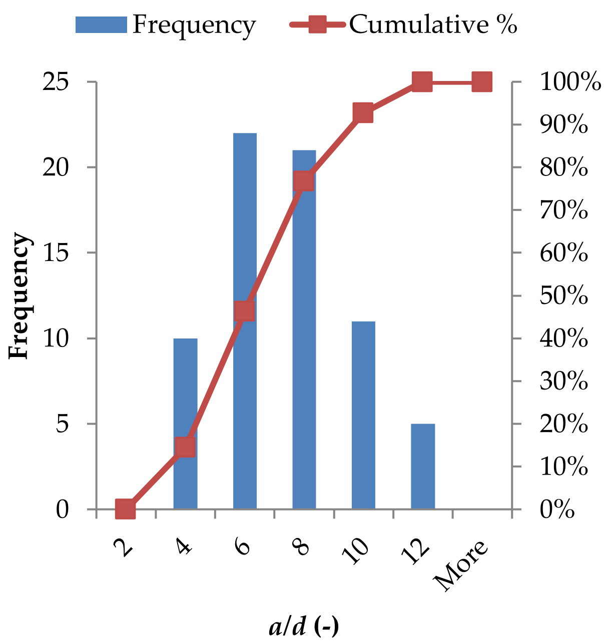

Figure 15. Distribution of the most important parameters in the database: (a) concrete compressive strength f_c; (b) tensile reinforcement ratio ρ; (c) effective depth d; (d) shear span to average effective depth ratio a/d.

3. Results

3.1 Parameter studies

The raw data from the database are used to analyze the effect of different experimental parameters on the sectional shear stress at failure as a result of the applied load. ACI 318-14 expression is used for determining v_u. Normalized shear stresses are used to discard the influence of the concrete compressive strength f_c. An analysis of the normalized shear stress to the square root and to the cube root is made. Figure 16 shows the relation between the normalized shear strength and f_c. From this figure, it can be seen that, for the studied experimental results, normalizing the shear strength to the square root is to be preferred. A similar observation was made for the shear capacity of steel fiber reinforced concrete beams [23].

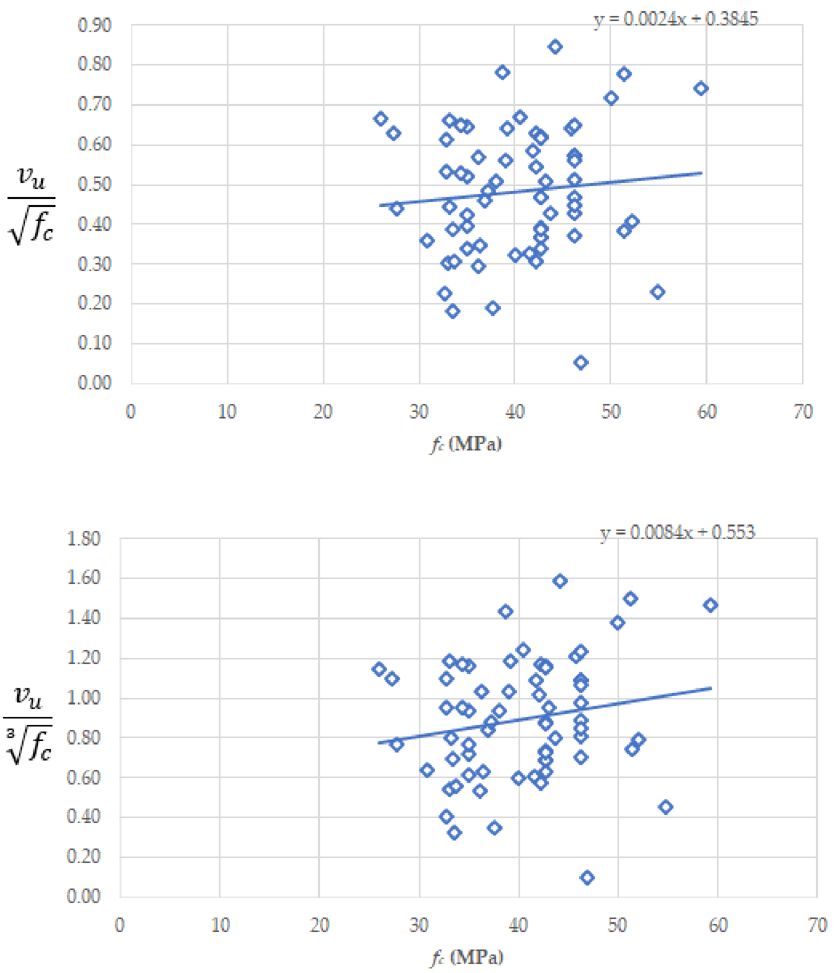

Figure 16. Normalized shear stresses to the concrete compressive strength: (a) normalized to the square root; (b) normalized to the cube root.

The influence of different parameters will be studied as a function of the shear stress normalized to the square root of f_c. Figure 17 shows the influence of the most important parameters on the shear stress normalized to the square root of f_c. Figure 17a shows the influence of the effective depth on the normalized shear stress. For the specimens in the compiled database, the effective depth has very little influence on the normalized shear stress. However, experiments on slabs with a larger effective depth are not available, so that this database cannot give insights regarding the size effect in eccentric punching shear. Figure 17b shows the influence of the reinforcement ratio ρ. Larger reinforcement ratios result in larger shear capacities, as expected. As more tension reinforcement is provided, the contribution of dowel action to the shear capacity increases, as reflected by the results from the database. Figure 17c shows the influence of the shear span to effective depth a/d. The shear capacity tends to decrease as a/d increases. This observation can be explained by the fact that for lower a/d ratios, direct load transfer between the point of application of the load and the support occurs. When direct load transfer occurs, the shear capacity is increased as a result of the shear-carrying mechanism of arching action.

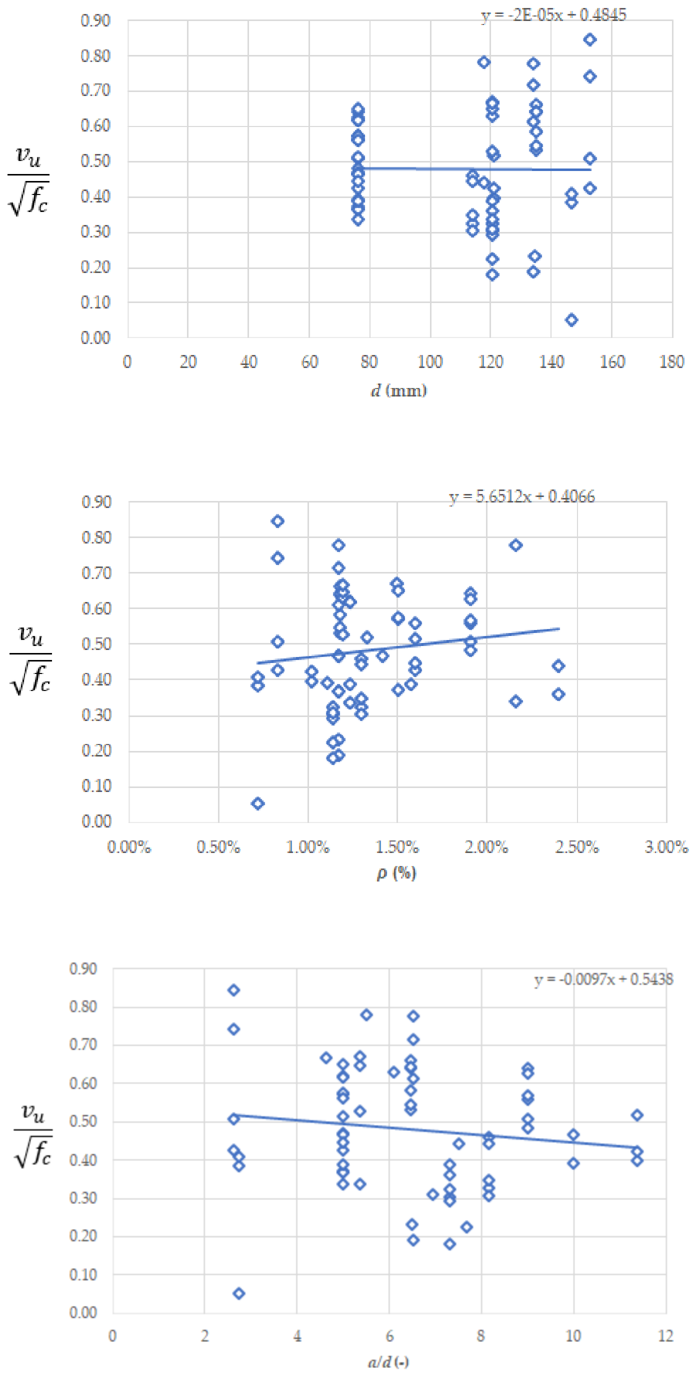

Figure 17. Parameter studies based on the normalized shear stress at failure of all entries in the database: (a) effective depth d; (b) longitudinal reinforcement ratio ρ; (c) shear span to depth ratio a/d.

3.2 Comparison to code predictions

The measured shear capacities from the database are then compared to the shear capacities predicted by four different models: ACI 318-14 [7], NEN-EN 1992-1-1:2005 [8], *fib* Model Code 2010 [9], and the Critical Shear Crack Theory [10,11]. Figure 18 shows the comparison between tested and predicted results, with the statistical properties of V_{test}/V_{pred} in Table 2. Results for all the entries of the database are presented in Table A6. Some entries do not present direct load applied to the slabs, only moment transferred from the column. In these references NEN-EN 1992-1-1:2005 [8], *fib* Model Code 2010 [9], and the Critical Shear Crack Theory [10,11] models were not evaluated. The validation of the spreadsheet used for calculating code predictions is available in the public domain [24]. Table 3 shows the statistical properties of V_{test}/V_{pred} only for slabs with shear reinforcement and Table 4 only for slabs without shear reinforcement. All references used in this database made code comparisons. Typically, the codes used were ACI 318-14 [7] and NEN-EN 1992-1-1:2005 [8] showing results similar to the ones presented in this study.

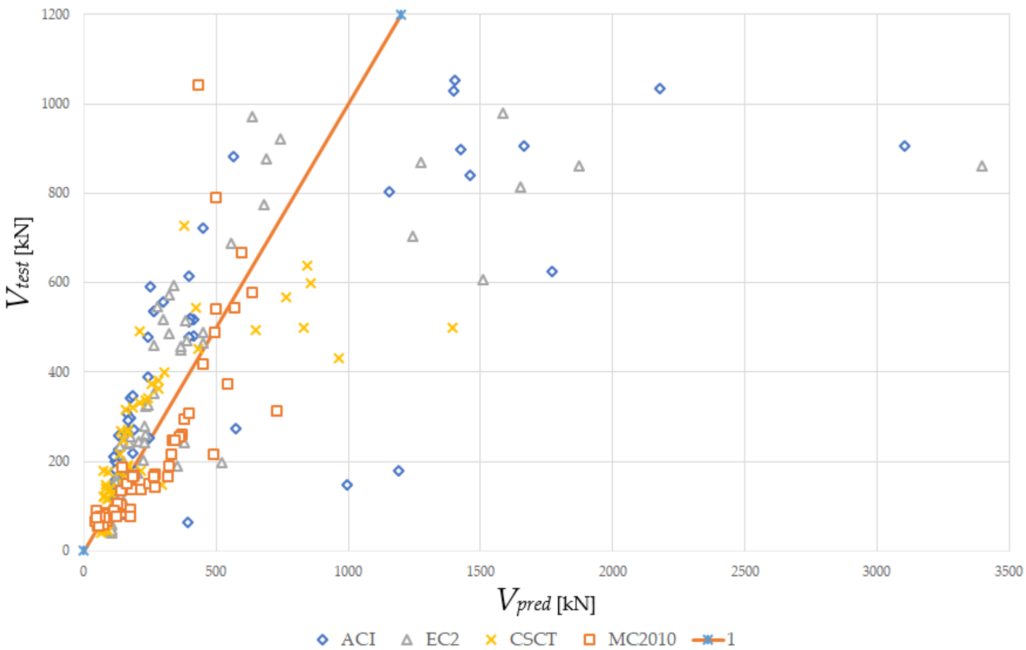

Figure 18. Comparison between experimental V_{test} and predicted shear capacities V_{pred} for 4 design methods from existing codes.

Table 2. Statistical properties of V_{test}/V_{pred} for all 70 datapoints

Model	AVG	STD	COV	min	max
ACI [7]	1.22	0.54	44%	0.15	2.37
EC2 [8]	1.04	0.4	41%	0.25	1.97
MC2010 [9]	1.25	0.39	34%	0.41	2.33
CSCT [10,11]	1.21	0.42	38%	0.36	2.37

Table 3. Statistical properties of V_{test}/V_{pred} for slabs with shear reinforcement

Model	AVG	STD	COV	min	max
ACI [7]	0.57	0.35	61%	0.15	1.56
EC2 [8]	0.74	0.39	53%	0.25	1.53
MC2010 [9]	1.11	0.45	41%	0.41	2.32
CSCT [10,11]	0.86	0.41	48%	0.36	1.92

Table 4. Statistical properties of V_{test}/V_{pred} for slabs without shear reinforcement

Model	AVG	STD	COV	min	max
ACI [7]	1.4	0.45	32%	0.2	2.4
EC2 [8]	1.1	0.40	35%	0.4	2.0
MC2010 [9]	1.3	0.43	32%	0.5	2.3
CSCT [10,11]	1.3	0.44	33%	0.5	2.4

4. Discussion

None of the codes presented highly conservative results, with average tested to predicted ratios between 1.04 and 1.25. The tested to predicted values using NEN-EN 1992-1-1:2005 [8] show the lower maximum value (for one entry) and the lowest average value, see Table 2. For the information in this database NEN-EN 1992-1-1:2005 [8] is the model that best predicts the capacity, although with a relatively large scatter (COV= 41%). The tested to predicted values using ACI 318-14 [7] show the lowest value for one entry, 0.15. Only using ACI 318-14 [7] the lowest value is this experiment. Whereas the other models consider only a part of the shear reinforcement, ACI 318-14 [7] considers all the reinforcement displaced on the peripheral line that is geometrically like the perimeter of the column section. As a result, this cause that the predicted shear resistance according to ACI 318-14 is significantly larger than the capacity predicted with the other methods.

Tables 3 and 4 show that the coefficient of variation for experiments without shear reinforcement are smaller than the ones with shear reinforcement. Models based on the Critical Shear Crack Theory don't present a big change, only empirical models such as ACI 318-14 [7] and NEN-EN 1992-1-1:2005 [8] show significantly larger scatters when analyzing only slabs with shear reinforcement.

High strength concrete slabs are not included in the study due to the lack of experiments on high-strength concrete slab-column connections. It would be interesting to investigate the behavior of this type of slabs in comparison with the ones considered for this study. Reference [25] presents a study on concentric experiments in high strength concrete slabs without shear reinforcement and concluded that the use of high strength concrete improves punching shear resistance.

In most cases, the results found in the literature indicate that there is an important reduction of the punching capacity when unbalanced moments occur in the slab column connection. Nevertheless, most databases, experiments and research focus on concentric punching shear. Models developed empirical equations that include the effect eccentricities by different methods such as critical perimeter reduction or increase of the applied shear stress, but there is not a mechanics-based model that is practical enough to be implemented in the construction codes. Mechanics-based models such as the Critical Shear Crack Theory are developed for the case of concentric punching shear and use simplified assumption for the extension to eccentric punching shear. For this database, the empirical methods showed large scatter on the results of the tested to predicted capacities, represented by the high coefficients of variation. This observation may be explained by the fact that all methods under consideration were originally developed for concentric punching shear, and validated with concentric punching sear tests, and then extended to the use of eccentric punching shear.

Realistic size slabs experiments in punching shear are not commonly found in the literature. None of the entries in this database is considered as a realistic size slab as none of these has an effective depth over 200 mm. Making this kind of experiments would represent the behavior of actual structures with a more realistic approach.

5. Conclusions

The lack of understanding regarding eccentric punching shear presents a practical problem because local forces typically control slab design. The transfer of unbalanced moments from the slab to the column cause an increase of the resulting shear stress. When this effect is not well-understood, as has happened in practice, it may lead to a punching failure of the slab-column connection and a possible collapse of the building. This study evaluates the available code provisions against 66 experimental results reported in the literature.

Analyzing the available experimental results from the database resulted in the following conclusions:

- All experiments are carried out in slabs under 200 mm depth. As such, the experiments cannot be used to evaluate the size effect in shear.
- There is a lack of experiments in eccentric punching shear.
- Most specimens have large reinforcement ratios to avoid a flexural failure before reaching the punching shear capacity of the slab.

- All specimens are cast using normal strength concrete.

The parameter studies led to the following observations:

- An analysis of the data showed that the shear stresses should be normalized to the square root of the concrete compressive strength. This ratio shows a smaller relation to concrete compressive strength than when shear stress is normalized to the cube root of the concrete compressive strength.
- The normalized shear strength increased as the reinforcement ratio increased. This influence was expected because a larger amount of reinforcement results in more dowel action, and thus a larger shear capacity.

From the comparison between the experimental shear capacities and the capacities predicted by the available codes, the following conclusion result:

- The average value of tested to predicted shear capacity is obtained with the Eurocode provisions. For the Eurocode provisions, however, the associated coefficient of variation is rather large (41%).
- The coefficient of variation of the tested to predicted shear capacities is lower for the expressions based on the Critical Shear Crack Theory than for the empirical expressions from Eurocode 2 and ACI 318.
- The coefficient of variation of the tested to predicted shear capacities is lower for the experiments without shear reinforcement than for the experiments with shear reinforcement.

A better understanding of eccentric punching shear and further experiments on deeper slabs and slabs with high-strength concrete are necessary to obtain save designs, optimize the design of building floors, and develop better tools for the assessment of existing building slabs.

Author Contributions: conceptualization, EOLL.; methodology, DV and EOLL.; software, DV; validation, KG and EOLL.; formal analysis, DV.; investigation, DV and EOLL; resources, EOLL; data curation, DV and EOLL; writing—original draft preparation, DV and EOLL; writing—review and editing, KG; visualization, DV; supervision, EOLL; project administration, EOLL; funding acquisition, EOLL.

Funding: This research is part of the program of Collaboration Grants 2019 of Universidad San Francisco de Quito. The APC was funded by the open access initiative of Delft University of Technology.

Acknowledgments: The authors would like to thank the program of Collaboration Grants 2019 of Universidad San Francisco de Quito for the financial support. We also would like to thank Prof. Regan for sharing his experimental results for this study.

Conflicts of Interest: The authors declare no conflict of interest.

List of notations

A_{sw}	area of the shear reinforcement for NEN-EN 1992-1-1:2005
A_v	area of the shear reinforcement in ACI 318-14
$C_{Rd,c}$	constant used for determining the shear capacity
E_s	modulus of elasticity of the steel
J_c	polar moment of inertia of the critical section
L_1	dimension of the loading plate
L_2	dimension of the loading plate
L_x	dimension of the slab
L_y	dimension of the slab
M_{Ed}	design moment
M_{mu}	model ultimate internal moment
M_u	factored moment applied on the slab
U_1	control perimeter for NEN-EN 1992-1-1:2005
U_1*	reduced critical control perimeter for NEN-EN 1992-1-1:2005
V_{Ed}	design shear strength
V_{Rd}	punching resistance for Model Code 2010

$V_{Rd,c}$ punching resistance provided by the concrete for Model Code 2010
$V_{Rd,s}$ punching resistance provided by the steel for Model Code 2010
V_u factored shear applied on the slab
V_{mu} model ultimate internal shear
W_{sup} width of the support
W_1 plastic modulus of control perimeter for NEN-EN 1992-1-1:2005
a shear span
a_v clear shear span
b_0 control perimeter for Model Code 2010
$b_{0,int}$ critical perimeter inside the shear reinforced zone for CSCT
b_1 dimension of the critical perimeter for NEN-EN 1992-1-1:2005
$b_{1,MC}$ basic control perimeter for Model Code 2010
b_2 dimension of the critical perimeter for Model Code 2010
b_o perimeter of the critical perimeter for ACI 318-14
b_u diameter of the circle with the same area as the region inside $b_{1,MC}$
b_y dimension on the critical perimeter U_1
b_z dimension on the critical perimeter U_1
c distance to the centroid of the critical perimeter
c_1 dimension of the column
c_2 dimension of the column
d average effective depth of the slab
d_g maximum aggregate size
d_v average effective depth of the slab for Model Code 2010
$d_{x,t}$ top longitudinal reinforcement in the x- axis
$d_{y,t}$ top longitudinal reinforcement in the y- axis
$d_{x,b}$ bottom longitudinal reinforcement in the x- axis
$d_{y,b}$ bottom longitudinal reinforcement in the y- axis
e eccentricity M/V
e_{par} eccentricity parallel to the edge of the slab
e_u eccentricity of the resultant forces
e_y eccentricity caused by a moment acting on the y- axis
e_z eccentricity caused by a moment acting on the x- axis
f_{bd} bond strength
f_c compressive strength of the concrete for ACI 318-14
f_{ck} compressive strength of the concrete for Model Code 2010
f_{ct} tensile strength of the concrete
f_{yt} yield strength of the reinforcement
f_{ywd} design yield strength of the shear reinforcement
$f_{ywd,ef}$ effective design strength of shear reinforcement
h depth of the slab
k size effect factor
k_c column size effect factor
k_{dg} coefficient of aggregate size
k_e coefficient of eccentricity
k_ψ coefficient of rotation
m_{rd} average flexural strength per unit length in the support strip
m_{sd} average moment per unit length for calculation flexural reinforcement in the support strip
r_s distance from column axis to line of contraflexure of the radial bending moments
m_{xD} model design moment on the x- axis.
m_{yD} model design moment on the y- axis
s_r radial spacing of the reinforcement

v_c	punching resistance provided by the concrete for ACI 318-14
v_{Ed}	design shear stress
v_n	nominal shear strength for ACI 318-14
$v_{Rd,\,c}$	shear resistance provided by the concrete
v_{Rd}	shear resistance for Model Code 2010 and CSCT
$v_{Rd,cs}$	shear resistance for NEN-EN 1992-1-1:2005
$v_{Rd\,s}$	shear resistance provided by the steel
v_s	punching resistance provided by the steel reinforcement for ACI 318-14
v_u	maximum shear stress for ACI 318-14
γ_f	fraction of the unbalanced moment transmitted by flexure
γ_v	fraction of the unbalanced moment transmitted by shear
α	angle between shear reinforcement and horizontal plane of the slab
α_s	constant used for determining shear capacity according to ACI 318-14
β	enhancement factor for eccentric shear
ρ_l	longitudinal steel reinforcement ratio
ρ_{ly}	longitudinal steel reinforcement ratio on the *y*- axis
ρ_{lx}	longitudinal steel reinforcement ratio on the *x*- axis
$\rho_{t,x}$	tensile steel reinforcement ratio on the *x*- axis
$\rho_{t,y}$	tensile steel reinforcement ratio on the *y*- axis
ρ_v	shear steel reinforcement ratio
σ_{swd}	shear reinforcement stress
ϕ_w	shear reinforcement diameter
ψ	rotation of the slab

References

1. Wight, J; MacGregor, J. Two-Way Slabs; Behavior, Analysis, and Design. *In Reinforced Concrete Mechanics & Design*, 6th ed.; Stark, H. Pearson: London, England, 2012, Volume 1, pp. 632-731.
2. Krüger, G; Burdet, O; Favre, R. Resistance au Poinconnement Excentre des Plancers Dalles. PhD dissertation, EPFL, Lausanne, Switzerland, 1999.
3. Muttoni, A; Fernandez, M; Simoes, J. The theoretical principles of the critical shear crack theory for punching shear failures and derivation of consistent close-form design expressions. Wiley, published. DOI: 10.1002/suco.201700088.
4. Punching of reinforced concrete slabs: Lessons learned from collapses and research. Available online: http://www.construction-conf.co.il/Portals/68/AurelioMuttoni.pdf (accessed on 29 of May of 2019).
5. Kinnunen, S., Nylander, H.: Punching of Concrete Slabs Without Shear Reinforcement, Transactions of the Royal Institute of Technology, No. 158, Stockholm, Sweden, 1960, p. 112.
6. Muttoni, A; Fernández, M. The Levels-of-Approximation approach in MC 2010: applications to punching shear provisions. *Structural Concrete. 2012*, Volume 13, pp. 32-41.
7. ACI Committee 318*. Building code requirements for structural concrete (ACI 318-14) and commentary*; American Concrete Institute: Farmington Hills, MI, 2014, pp.100.
8. European Committee for Standardization.; British Standards Institution. *Eurocode 2: design of concrete structures;* British Standards Institution: London, 2004, pp. 97.
9. *fib. Model code 2010: final draft*; International Federation for Structural Concrete: Lausanne, 2012; pp. 382.
10. Fernández, M.; Muttoni, A. Application of Critical Shear Crack Theory to Punching of Reinforced Concrete Slabs with Transverse Reinforcement. *ACI Structural Journal* 2009, 106.
11. Muttoni, A. Punching Shear Strength of Reinforced Concrete Slabs without Transverse Reinforcement. *ACI Structural Journal* 2008, 105.
12. Moe, J. Shearing Strength of Reinforced Concrete Slabs and Footings under Concentrated Loads, Development Department Bulletin D47, Portland Cement Association, Skokie, IL., April 1961.
13. ACI-ASCE Committee 426, "The Shear Strength of Reinforced Concrete Members," Chapter 5, "Shear Strength of Slabs," Proceedings ASCE, Journal of the Structural Division, Vol. 100, No. ST8, August 1974, pp. 1543–1591.
14. Albuquerque, N; Melo, G; Vollum, R. Punching Shear Strength of Flat Slab-Edge Column Connections with Outward Eccentricity of Loading. *ACI Structural Journal* 2016, 113.
15. Hammill, N; Ghali, A. Punching Shear Resistance of Corner Slab-Column Connections. ACI Structural Journal 1994, 91.
16. Narashiman, N. Shear reinforcement in reinforced concrete column heads. Thesis, Doctor of Philosophy in the Faculty of Engineering, Imperial College of Science and Technology, London, 1971.
17. Zaghlool, E. Strength and behaviour of corner and edge column-slab connections in reinforced concrete flat plates. Thesis, Doctor of philosophy in Civil Engineering, University of Calgary, Calgary, 1971.
18. Anis, N. Shear strength of reinforced concrete flat slabs without shear reinforcement. Thesis, Doctor of Philosophy in the Faculty of Engineering, Imperial College of Science and Technology, London, 1970.
19. Tankut, A. The behaviour of the reinforced concrete flat plate structures subjected to various combinations of vertical and horizontal loads. Thesis, Doctor of Philosophy in the Faculty of Engineering, Imperial College of Science and Technology, London, 1969.
20. Vargas, D. Database of experiments on eccentric punching shear on flat slabs; Zenodo, Ed. 2019; 10.5281/zenodo.2655094.
21. Sarveghadi, M.; Gandomi, A.H.; Bolandi, H.; Alavi, A.H. Development of prediction models for shear strength of SFRCB using a machine learning approach. Neural Computing and Applications 2015, 10.1007/s00521-015-1997-6, doi:10.1007/s00521-015-1997-6.
22. SCIA Downloads. Available online: https://www.scia.net/en/support/downloads (accessed on 28 of May 2019).
23. Lantsoght, E. Database of Shear Experiments on Steel Fiber Reinforced Concrete Beams without Stirrups. Materials 2019, 12(6), 917; https://doi.org/10.3390/ma12060917.
24. Vargas, D. Validation of spreadsheet for database of experiments on eccentric punching shear on flat slabs; Zenodo, Ed. 2019; 10.5281/zenodo.2655096.
25. D. Tuan Ngo. Punching shear resistance of high-strength concrete slabs. Electronic Journal of Structural Engineering, 2001, 1.

Appendix A

Table A1. Database Part I

Reference	Slab	Type	Slab geometry						
			L_x (mm)	L_y (mm)	h (mm)	$d_{x,t}$ (mm)	$d_{y,t}$ (mm)	$d_{x,b}$ (mm)	$d_{y,b}$ (mm)
ALBUQUERQUE [14]	L1	EDG	2350	1700	180	140	154	141	152
	L5	EDG	2350	1700	180	140	154	141	152
	L6	EDG	2350	1700	180	140	154	141	152
	L10	EDG	2350	1700	180	140	154	154	152
	L11	EDG	2350	1700	180	140	154	154	152
	L12	EDG	2350	1700	180	140	154	154	152
	L13	EDG	2350	1700	180	140	154	154	152
KRÜGER [2]	P16A	INT	3000	3000	150	-	-	121	121
	P30A	INT	3000	3000	150	-	-	121	121
	PP16B	INT	3000	3000	150	-	-	121	121
HAMMILL & GHALI [15]	NH1	CNR	1075	1075	150	114	114	114	114
	NH2	CNR	1075	1075	150	114	114	114	114
	NH3	CNR	1075	1075	150	114	114	114	114
	NH4	CNR	1075	1075	150	114	114	114	114
	NH5	CNR	1075	1075	150	114	114	114	114
NARASHIMAN [16]	L1	INT	2280	2280	178	135	135	135	135
	L3	INT	2280	2280	178	135	135	135	135
	L4	INT	2280	2280	178	135	135	135	135
	L5	INT	2280	2280	178	135	135	135	135
	L6	INT	2280	2280	178	135	135	135	135
	L10	INT	2280	2280	178	135	135	135	135
	ES2	EDG	1295	2280	178	134	134	134	134
	ES3	EDG	1295	2280	178	134	134	134	134
	ES4	EDG	1295	2280	178	134	134	134	134
	ES5	EDG	1295	2280	178	134	134	134	134
	ES7	EDG	1295	2280	178	134	135	134	134
ZAGHLOOL [17]	Z-I (1)	CNR	1067	1067	152	121	121	121	121
	Z-II(1)	CNR	1067	1067	152	121	121	121	121
	Z-II(2)	CNR	1067	1067	152	121	121	121	121
	Z-II(3)	CNR	1067	1067	152	118	118	118	118
	Z-II(4)	CNR	1067	1067	152	121	121	121	121
	Z-II(6)	CNR	1067	1067	152	121	121	121	121
	Z-II(7)	CNR	1067	1067	152	121	121	121	121
	Z-II(8)	CNR	1067	1067	152	121	121	121	121
	Z-III(1)	CNR	1067	1067	152	121	121	121	121
	Z-IV(1)	EDG	1829	965	152	121	121	121	121
	Z-V(1)	EDG	1829	965	152	121	121	121	121
	Z-V(2)	EDG	1829	965	152	121	121	121	121
	Z-V(3)	EDG	1829	965	152	118	118	118	118
	Z-V(4)	EDG	1829	965	152	121	121	121	121
	Z-V(6)	EDG	1829	965	152	121	121	121	121
	Z-VI(1)	EDG	1829	965	152	121	121	121	121
ANNIS [18]	B.1	INT	1524	1524	102	76	76	76	76

	B.3	INT	1524	1524	102	76	76	76	76
	B.4	INT	1524	1524	102	76	76	76	76
	B.5	INT	1524	1524	102	76	76	76	76
	B.6	INT	1524	1524	102	76	76	76	76
	B.7	INT	1524	1524	102	76	76	76	76
TANKUT [19]	E.1	INT	1524	1524	102	71	81	81	71
	E.2	INT	1524	1524	102	71	81	81	71
	B.1	EDG	1524	762	102	71	81	81	71
	B.2	EDG	1524	762	102	71	81	81	71
	H.1	EDG	1524	762	102	71	81	81	71
	H.2	EDG	1524	762	102	71	81	81	71
	D.1	EDG	762	1524	102	71	81	81	71
	D.2	EDG	762	1524	102	71	81	81	71
	F.1	EDG	762	1524	102	71	81	81	71
	F.2	EDG	762	1524	102	71	81	81	71
	A.1	CNR	762	762	102	71	81	81	71
	A.2	CNR	762	762	102	71	81	81	71
	C.1	CNR	762	762	102	71	81	81	71
	C.2	CNR	762	762	102	71	81	81	71
	G.1	CNR	762	762	102	71	81	81	71
	G.2	CNR	762	762	102	71	81	81	71
	K.1	CNR	762	762	102	71	81	81	71
	K.2	CNR	762	762	102	71	81	81	71

Table A2. Database Part II

Reference	Slab	Type	Longitudinal reinforcement					Concrete properties				
			$\rho_{t,x}$ (%)	$\rho_{t,y}$ (%)	ρ (%)	f_y (MPa)	E_s (GPa)	Age (days)	f_c (MPa)	f_{ct} (MPa)	Test f_{ct}	d_g (mm)
ALBUQUERQUE [14]	L1	EDG	0.44%	1.17%	0.72%	544	192	28	47	3.4	CS	9.5
	L5	EDG	0.44%	1.17%	0.72%	544	192	28	51	4.1	CS	9.5
	L6	EDG	0.44%	1.17%	0.72%	544	192	28	52	4.3	CS	9.5
	L10	EDG	0.44%	1.56%	0.83%	544	192	28	59	3.6	CS	9.5
	L11	EDG	0.44%	1.56%	0.83%	544	192	28	43	3.1	CS	9.5
	L12	EDG	0.44%	1.56%	0.83%	544	192	28	44	3.3	CS	9.5
	L13	EDG	0.44%	1.56%	0.83%	544	192	28	44	3.4	CS	9.5
KRÜGER [2]	P16A	INT	1.02%	1.02%	1.02%	480	200	28	35	4.67	S	9.5
	P30A	INT	1.02%	1.02%	1.02%	480	200	28	35	4.67	S	9.5
	PP16B	INT	1.33%	1.33%	1.33%	480	200	28	35	4.67	S	9.5
HAMMILL & GHALI [15]	NH1	CNR	1.30%	1.30%	1.30%	440	200	28	42	5.09	S	9.5
	NH2	CNR	1.30%	1.30%	1.30%	440	200	28	42	5.13	S	9.5
	NH3	CNR	1.30%	1.30%	1.30%	440	200	28	36	4.77	S	9.5
	NH4	CNR	1.30%	1.30%	1.30%	440	200	28	37	4.80	S	9.5
	NH5	CNR	1.30%	1.30%	1.30%	440	200	28	33	4.55	S	9.5
NARASHIMAN [16]	L1	INT	1.18%	1.18%	1.18%	398	200	28	33	2.7	CS	19
	L3	INT	1.18%	1.18%	1.18%	398	200	28	33	5.66	CS	19
	L4	INT	1.18%	1.18%	1.18%	398	200	28	46	3.45	CS	19
	L5	INT	1.18%	1.18%	1.18%	398	200	28	35	2.98	CS	19
	L6	INT	1.18%	1.18%	1.18%	398	200	28	42	3.07	CS	19
	L10	INT	1.18%	1.18%	1.18%	398	200	28	42	2.47	CS	19
	ES2	EDG	1.16%	1.18%	1.17%	398	200	28	33	2.7	CS	19
	ES3	EDG	1.16%	1.18%	1.17%	398	200	28	51	3.1	CS	19
	ES4	EDG	1.16%	1.18%	1.17%	398	200	28	50	3.31	CS	19
	ES5	EDG	1.16%	1.18%	1.17%	398	200	28	38	2.63	CS	19
	ES7	EDG	1.16%	1.18%	1.17%	398	200	28	55	3.38	CS	19
ZAGHLOOL [17]	Z-I (1)	CNR	1.23%	1.05%	1.14%	379	200	28	33	3.83	CS	12.5
	Z-II(1)	CNR	1.23%	1.05%	1.14%	389	200	28	33	3.63	CS	12.5
	Z-II(2)	CNR	1.76%	1.41%	1.57%	405	200	28	33	3.83	CS	12.5
	Z-II(3)	CNR	2.56%	2.24%	2.40%	451	200	28	28	3.87	CS	12.5
	Z-II(4)	CNR	1.23%	1.05%	1.14%	389	200	28	31	3.36	CS	12.5
	Z-II(6)	CNR	1.23%	1.05%	1.14%	381	200	28	34	3.04	CS	12.5
	Z-II(7)	CNR	1.23%	1.05%	1.14%	382	200	28	40	3.81	CS	12.5
	Z-II(8)	CNR	1.23%	1.05%	1.14%	382	200	28	36	3.50	CS	12.5
	Z-III(1)	CNR	1.23%	1.05%	1.14%	379	200	28	34	3.94	CS	12.5
	Z-IV(1)	EDG	1.13%	1.26%	1.19%	476	200	28	27	2.99	CS	12.5
	Z-V(1)	EDG	1.13%	1.26%	1.19%	474	200	28	34	3.52	CS	12.5
	Z-V(2)	EDG	1.64%	1.36%	1.49%	474	200	28	40	3.61	CS	12.5
	Z-V(3)	EDG	2.22%	2.10%	2.16%	475	200	28	39	3.79	CS	12.5
	Z-V(4)	EDG	1.13%	1.26%	1.19%	437	200	28	35	4.10	CS	12.5
	Z-V(6)	EDG	1.13%	1.26%	1.19%	476	200	28	34	3.63	CS	12.5
	Z-VI(1)	EDG	1.13%	1.26%	1.19%	476	200	28	26	2.83	CS	12.5
ANNIS [18]	B.1	INT	1.90%	1.90%	1.90%	330	205	28	39	4.94	S	9.5
	B.3	INT	1.90%	1.90%	1.90%	330	205	28	38	4.87	S	9.5

	B.4	INT	1.90%	1.90%	1.90%	330	205	28	37	4.82	S	9.5
	B.5	INT	1.90%	1.90%	1.90%	330	205	28	36	4.75	S	9.5
	B.6	INT	1.90%	1.90%	1.90%	330	205	28	39	4.94	S	9.5
	B.7	INT	1.90%	1.90%	1.90%	330	205	28	42	5.13	S	9.5
TANKUT [19]	E.1	INT	1.18%	1.04%	1.11%	404	169	28	43	5.16	S	9.5
	E.2	INT	1.51%	1.33%	1.41%	310	184	28	46	5.37	S	9.5
	B.1	EDG	1.18%	1.15%	1.17%	404	169	28	43	5.16	S	9.5
	B.2	EDG	1.51%	1.50%	1.50%	310	184	28	46	5.37	S	9.5
	H.1	EDG	1.18%	1.15%	1.17%	404	169	28	43	5.16	S	9.5
	H.2	EDG	1.51%	1.50%	1.50%	310	184	28	46	5.37	S	9.5
	D.1	EDG	1.31%	1.04%	1.17%	404	169	28	43	5.16	S	9.5
	D.2	EDG	1.70%	1.33%	1.50%	310	184	28	46	5.37	S	9.5
	F.1	EDG	1.31%	1.04%	1.17%	404	169	28	43	5.16	S	9.5
	F.2	EDG	1.70%	1.33%	1.50%	310	184	28	46	5.37	S	9.5
	A.1	CNR	1.31%	1.15%	1.23%	404	169	28	43	5.16	S	9.5
	A.2	CNR	1.70%	1.50%	1.60%	310	184	28	46	5.37	S	9.5
	C.1	CNR	1.31%	1.15%	1.23%	404	169	28	43	5.16	S	9.5
	C.2	CNR	1.70%	1.50%	1.60%	310	184	28	46	5.37	S	9.5
	G.1	CNR	1.31%	1.15%	1.23%	404	169	28	43	5.16	S	9.5
	G.2	CNR	1.70%	1.50%	1.60%	310	184	28	46	5.37	S	9.5
	K.1	CNR	1.31%	1.15%	1.23%	404	169	28	43	5.16	S	9.5
	K.2	CNR	1.70%	1.50%	1.60%	310	184	28	46	5.37	S	9.5

CS for Cylinder Split and S for using the Sarveghadi formula Eq. (44) for obtaining f_{ct}

Table A3. Database Part III

Reference	Id	Support geometry					Loading			
		L_1 (mm)	L_2 (mm)	a (mm)	av (mm)	W_{sup} (mm)	$M_{u,x}$ (kNm)	$M_{u,y}$ (kNm)	V_u (kN)	Failure Mode
ALBUQUERQUE [14]	L1	100	100	400	200	300	-	-95	437	PUNCH
	L5	100	100	400	200	300	-	38	654	PUNCH
	L6	100	100	400	200	300	-	67	605	PUNCH
	L10	100	100	400	200	300	-	90	815	PUNCH
	L11	100	100	400	200	300	-	112	615	PUNCH
	L12	100	100	400	200	300	-	56	655	PUNCH
	L13	100	100	400	200	300	-	127	700	PUNCH
KRÜGER [2]	P16A	300	300	1375	1100	250	-	53	331	PUNCH
	P30A	300	300	1375	1100	250	-	86	270	PUNCH
	PP16B	300	300	1375	1100	250	-	69	432	F. PUNCH
HAMMILL & GHALI [15]	NH1	250	250	930	785	40	43	-43	147	PUNCH
	NH2	250	250	930	785	40	40	-40	139	PUNCH
	NH3	250	250	930	785	40	41	-41	147	PUNCH
	NH4	250	250	930	785	40	33	-33	0	PUNCH
	NH5	250	250	930	785	40	56	-56	179	PUNCH
NARASHIMAN [16]	L1	305	305	874	715	13	-	122	399	PUNCH
	L3	305	305	874	715	13	-	152	499	PUNCH
	L4	305	305	874	715	13	-	173	568	PUNCH
	L5	305	305	874	715	13	-	152	499	PUNCH
	L6	305	305	874	715	13	-	91	598	PUNCH
	L10	305	305	874	715	13	-	97	638	PUNCH
	ES2	305	305	874	715	13	-	78	342	PUNCH
	ES3	305	305	874	715	13	-	124	543	PUNCH
	ES4	305	305	874	715	13	-	113	495	PUNCH
	ES5	305	305	874	715	13	-	-112	492	PUNCH
	ES7	305	305	874	715	13	-	-166	728	PUNCH
ZAGHLOOL [17]	Z-I (1)	178	178	928	789	100	19	-19	74	PUNCH
	Z-II(1)	267	267	883	700	100	39	-39	138	PUNCH
	Z-II(2)	267	267	883	700	100	53	-53	177	PUNCH
	Z-II(3)	267	267	883	700	100	58	-58	178	PUNCH
	Z-II(4)	267	267	883	700	100	28	-28	0	PUNCH
	Z-II(6)	267	267	883	700	100	39	-39	82	PUNCH
	Z-II(7)	267	267	883	700	100	29	-29	0	PUNCH
	Z-II(8)	267	267	883	700	100	39	-39	139	PUNCH
	Z-III(1)	356	356	839	611	100	53	-53	180	PUNCH
	Z-IV(1)	178	178	735	597	100	48	-	122	PUNCH
	Z-V(1)	267	267	647	463	100	85	-	215	PUNCH
	Z-V(2)	267	267	647	463	100	94	-	247	PUNCH
	Z-V(3)	267	267	647	463	100	104	-	268	PUNCH
	Z-V(4)	267	267	647	463	100	81	-	0	PUNCH
	Z-V(6)	267	267	647	463	100	88	-	117	PUNCH
	Z-VI(1)	356	356	558	330	100	107	-	265	PUNCH
ANNIS [18]	B.1	203	203	686	508	152	-	71	0	F.PUNCH
	B.3	203	203	686	508	152	-	18	191	PUNCH

	B.4	203	203	686	508	152	-	26	140	PUNCH
	B.5	203	203	686	508	152	-	39	125	PUNCH
	B.6	203	203	686	508	152	-	54	116	PUNCH
	B.7	203	203	686	508	152	-	66	70	F.PUNCH
TANKUT [19]	E.1	203	203	762	660	0	1	12	165	PUNCH
	E.2	203	203	762	660	0	0	20	186	PUNCH
	B.1	203	203	381	279	0	0	25	88	PUNCH
	B.2	203	203	381	279	0	0	38	121	PUNCH
	H.1	203	203	381	279	0	1	27	76	PUNCH
	H.2	203	203	381	279	0	0	20	75	PUNCH
	D.1	203	203	381	279	0	11	6	74	PUNCH
	D.2	203	203	381	279	0	21	17	80	PUNCH
	F.1	203	203	381	279	0	11	6	74	PUNCH
	F.2	203	203	381	279	0	22	16	80	PUNCH
	A.1	305	305	381	229	0	17	14	48	PUNCH
	A.2	305	305	381	229	0	26	23	49	PUNCH
	C.1	305	305	381	229	0	13	12	46	PUNCH
	C.2	305	305	381	229	0	25	26	59	PUNCH
	G.1	305	305	381	229	0	22	35	54	PUNCH
	G.2	305	305	381	229	0	13	27	41	PUNCH
	K.1	305	305	381	229	0	23	34	54	PUNCH
	K.2	305	305	381	229	0	14	26	46	PUNCH

Table A4. Shear reinforcement.

Reference	Id	Shear reinforcement						
		Shear Reinforcement	ρ_v (%)	n_{bars}	ϕ (mm)	S_v (mm)	f_{ywd} (MPa)	A_{sw} (mm2)
ALBUQUERQUE [14]	L10	Studs	0.08%	28	8	150	587	1407
	L13	Stirrups	0.17%	24	8	60	587	1206
KRÜGER [2]	PP16B	Stirrups	0.36%	48	10	120	480	7540
HAMMILL & GHALI [15]	NH3	Studs	0.08%	12	10	57	440	942
	NH5	Studs	0.09%	20	10	85	440	1571
NARASHIMAN [16]	L3	Shear hat	0.18%	24	9.5	52	309	1710
	L4	Shear hat	0.18%	24	6.5	52	238	1710
	L5	Shear hat	0.31%	24	13	52	355	3040
	L6	Shear hat	0.12%	24	8	52	366	1190
	L10	Shear hat	0.12%	24	8	52	355	1190
	ES3	Shear hat	0.05%	16	6.5	52	238	517
	ES4	Shear hat	0.12%	16	9.8	52	309	1140
	ES7	Shear hat	0.05%	16	6.5	52	238	517

Table A5. SCIA Model results.

Reference	Id	M_{mux} (kNm)	M_{muy} (kNm)	V_{mux} (kN)	V_{muy} (kN)	m_{xD} (kNm)	m_{yD} (kNm)
ALBUQUERQUE [14]	L1	152	136	637	267	173	157
	L5	341	145	1069	460	430	234
	L6	193	221	913	387	261	290
	L10	487	194	1496	657	572	279
	L11	212	195	898	379	243	227
	L12	333	147	1055	453	432	246
	L13	339	165	1109	475	461	287
KRÜGER [2]	P16A	26	27	140	134	33	31
	P30A	22	24	127	116	27	28
	PP16B	34	35	182	173	42	40
HAMMILL & GHALI [15]	NH1	85	85	264	264	113	113
	NH2	80	80	251	251	106	106
	NH3	84	84	266	266	110	110
	NH4	30	30	114	114	44	44
	NH5	105	105	219	219	141	141
NARASHIMAN [16]	L1	65	69	530	349	63	76
	L3	79	86	663	436	79	95
	L4	90	98	754	497	90	108
	L5	79	86	663	436	79	95
	L6	80	103	659	523	80	108
	L10	85	110	703	558	85	116
	ES2	63	134	204	630	83	191
	ES3	100	212	325	1001	131	304
	ES4	91	193	296	911	119	276
	ES5	105	399	134	1776	219	526
	ES7	155	590	198	2627	324	779
ZAGHLOOL [17]	Z-I (1)	45	45	149	149	57	57
	Z-II(1)	78	78	248	248	102	102
	Z-II(2)	102	102	312	312	136	136
	Z-II(3)	104	104	305	305	142	142
	Z-II(4)	26	26	99	99	38	38
	Z-II(6)	52	52	120	120	80	80
	Z-II(7)	26	26	102	102	39	39
	Z-II(8)	84	84	226	226	120	120
	Z-III(1)	94	94	287	287	125	125
	Z-IV(1)	32	30	232	136	32	34
	Z-V(1)	53	50	359	233	53	50
	Z-V(2)	59	57	425	262	59	63
	Z-V(3)	65	62	454	287	65	67
	Z-V(4)	59	69	309	109	72	69
	Z-V(6)	74	156	300	301	115	156
	Z-VI(1)	61	58	376	280	61	58
ANNIS [18]	B.1	1	5	117	79	16	18
	B.3	32	32	285	256	41	34
	B.4	26	25	230	187	33	29

	B.5	24	23	232	169	31	33
	B.6	22	20	243	162	30	35
	B.7	13	12	202	135	26	26
TANKUT [19]	E.1	29	28	253	221	36	29
	E.2	33	32	288	249	42	33
	B.1	43	32	417	82	52	43
	B.2	61	44	585	116	72	60
	H.1	38	27	372	76	45	28
	H.2	36	28	350	59	44	36
	D.1	25	29	65	294	31	39
	D.2	20	24	91	276	31	35
	F.1	25	29	65	294	31	39
	F.2	20	24	90	282	31	36
	A.1	26	25	72	88	35	34
	A.2	28	31	46	58	51	52
	C.1	24	24	82	91	34	34
	C.2	35	33	78	73	58	57
	G.1	40	27	83	57	67	55
	G.2	33	17	79	34	53	37
	K.1	38	29	77	54	66	56
	K.2	34	20	87	30	54	40

Table A6. Code comparisons.

Reference	Slab	EC2	ACI	MC2010	CSCT
		V_{test}/V_{pred}	V_{test}/V_{pred}	V_{test}/V_{pred}	V_{test}/V_{pred}
ALBUQUERQUE [14]	L1	0.5	0.2	1.9	2.0
	L5	1.2	1.2	1.3	1.4
	L6	1.2	1.2	1.4	1.4
	L10	1.5	0.7	1.1	1.0
	L11	1.3	1.5	1.7	1.7
	L12	1.2	1.3	1.4	1.5
	L13	1.2	0.5	1.4	1.3
KRÜGER [2]	P16A	1.0	1.2	1.5	1.6
	P30A	1.1	1.3	1.6	1.6
	PP16B	0.4	0.4	0.4	0.4
HAMMILL & GHALI [15]	NH1	1.3	1.0	1.7	1.8
	NH2	1.3	0.9	1.6	1.6
	NH3	0.4	0.1	0.8	0.5
	NH4	-	1.4	-	-
	NH5	0.6	0.2	1.3	0.8
NARASHIMAN [16]	L1	1.2	1.6	1.3	1.3
	L3	0.5	0.5	0.9	0.6
	L4	0.6	0.7	1.0	0.7
	L5	0.3	0.3	0.6	0.4
	L6	0.5	0.6	0.9	0.7
	L10	0.7	0.6	1.1	0.8
	ES2	1.5	1.9	1.4	1.4
	ES3	1.1	1.6	1.5	1.3
	ES4	0.6	0.7	1.0	0.8
	ES5	1.8	0.6	2.3	2.3
	ES7	1.3	0.5	2.3	1.9
ZAGHLOOL [17]	Z-I (1)	0.8	0.7	1.2	1.2
	Z-II(1)	1.3	0.9	1.4	1.4
	Z-II(2)	1.5	1.2	1.9	1.9
	Z-II(3)	1.4	1.3	2.3	2.4
	Z-II(4)	-	1.1	-	-
	Z-II(6)	0.8	0.5	1.1	1.1
	Z-II(7)	-	1.0	-	-
	Z-II(8)	1.2	0.9	1.3	1.4
	Z-III(1)	1.5	0.9	1.3	1.3
	Z-IV(1)	1.2	1.9	1.6	1.6
	Z-V(1)	1.7	2.0	1.6	1.6
	Z-V(2)	1.7	2.0	1.6	1.7
	Z-V(3)	1.8	2.4	1.9	1.9
	Z-V(4)	-	1.0	-	-
	Z-V(6)	1.3	1.6	1.3	1.3
	Z-VI(1)	2.0	2.0	1.6	1.6
ANNIS [18]	B.1	-	1.7	-	-
	B.3	1.1	1.5	1.1	1.2
	B.4	1.0	1.5	1.0	1.1

	B.5	1.2	1.7	1.2	1.2
	B.6	1.4	1.9	1.3	1.3
	B.7	1.4	1.9	1.2	1.2
TANKUT [19]	E.1	0.9	1.2	1.1	1.1
	E.2	0.9	1.4	1.1	1.1
	B.1	1.3	1.4	1.3	1.3
	B.2	1.7	2.0	1.6	1.6
	H.1	1.3	1.4	1.3	1.3
	H.2	1.0	1.1	0.9	0.9
	D.1	0.9	1.1	0.9	0.9
	D.2	1.0	1.7	1.1	1.1
	F.1	0.9	1.1	0.9	0.9
	F.2	1.1	1.7	1.1	1.1
	A.1	0.5	1.2	0.6	0.6
	A.2	0.5	1.6	0.7	0.7
	C.1	0.5	1.0	0.5	0.5
	C.2	0.6	1.7	0.8	0.8
	G.1	0.6	1.9	1.0	1.0
	G.2	0.4	1.3	0.6	0.6
	K.1	0.6	1.9	1.0	0.9
	K.2	0.4	1.4	0.6	0.6
Average		1.04	1.22	1.25	1.21
Coefficient of variation		41%	44%	34%	38%
Standard Derivation		0.43	0.53	0.42	0.46